School of Mechanical Engineering

Faculty of Engineering

The University of New South Wales

Constructing a More Realistic Numerical Model of Idealized and Patient Specific Coronary Artery Based on Two-Way FSI and CFD Simulation

Author: Jiacheng Min

Submitted: 19/Nov/2021 Student zID: z5185479

Supervisor: Dr Susann Beier (UNSW)

ORIGINALITY STATEMENT

‘I hereby declare that this submission is my own work and to the best of my knowledge it contains no materials previously published or written by another person, or substantial proportions of material which have been accepted for the award of any other degree or diploma at UNSW or any other educational institution, except where due acknowledgement is made in the thesis. Any contribution made to the research by others, with whom I have worked at UNSW or elsewhere, is explicitly acknowledged in the thesis. I also declare that the intellectual content of this thesis is the product of my own work, except to the extent that assistance from others in the project's design and conception or in style, presentation and linguistic expression is acknowledged.’

Signed Jiacheng Min

Date 19/11/2021

Abstract

The cardiovascular diseases caused by the formation of atherosclerosis has become more and more severe in the past few years. Although some cardiovascular devices used in percutaneous coronary intervention can treat most of them in a short term, several devices can negatively affect the hemodynamics around the lesion, eventually resulting in the occur of adverse events. Therefore, constructing realistic and accurate numerical model for analyzing the hemodynamics can assist R&D engineers of cardiovascular devices to optimize their products for alleviating late adverse events. Total 19 successful FSI and CFD simulations with three different geometries have been conducted to identify the most realistic and accurate numerical model. The effects of outlet boundary condition, arterial wall deformation, material model, arterial wall structure on hemodynamic parameters has been evaluated. The key finding is that FSI method is more appropriate for investigating arterial hemodynamics.

Acknowledgements

I would like to thank my supervisor, Dr Susann Beier for the guidance on biomedical knowledge and the direction of thesis topic. I would like to thank my co-supervisor, Darson who gives me assistance in using FLUENT and conducting FSI simulation. I would like to thank Mr Behzad Babaei and professor Gangadhara Prusty for providing the basic principle of anisotropic hyperelastic material in ANSYS. I would also like to thank Mr Ramtin Gharleghi, Vamsi Krishnaa Ravi Kumar, Joshua Najdzion and Chi shen for their helps on using Katana, alleviating issues and editing report. I would also like to thank my girlfriend Zihui Kang who has always supported me.

Due to the traveling restriction, the author fully finishes this study in China. In addition, this study is completed without the use of KATANA because of the instable connection of UNSW VPN. Finally, I would like to thank the workstation provided by Lepu Mecial Company to let me run the FSI simulations.

Contents

List of Figures

List of Tables

Nomenclature

Abbreviations

BMS	Bare-Metal Stent
CAD	Coronary Artery Disease
CFD	Computational Fluid Dynamics
DES	Drug-Eluting Stents
FEA	Finite Element Analysis
FSI	Fluid Solid Interaction
ISR	In-Stent Restenosis
OSI	Oscillatory Shear Index
PCI	Percutaneous Coronary Intervention
ST	Stent Thrombosis
TAWSS	Time Averaged Wall Shear Stress
WSS	Wall Shear Stress

Mooney-Rivlin Equation Variables

C_{10}	Mooney-Rivlin Coefficient
C_{01}	Mooney-Rivlin Coefficient
C_{20}	Mooney-Rivlin Coefficient
C_{11}	Mooney-Rivlin Coefficient
C_{02}	Mooney-Rivlin Coefficient
D_1	Incompressible Parameter
$\overline{I_1}$	Stain Invariants
$\overline{I_2}$	Stain Invariants
W	Strain-Energy Potential
λ_1	Principal Stretch
λ_2	Principal Stretch
λ_3	Principal Stretch
μ_∞	Infinite-Shear Viscosity
ν	Poisson's Ratio

Carreau-Yasuda Viscosity Model Variables

n	Power Index
q	Yasuda Exponent
$\dot{\gamma}$	Shear Strain Rate
λ	Time Constant
μ	Variation of Viscosity
μ_0	Zero-Shear Viscosity

Anisotropic Hyperelastic Material Variables

$\boldsymbol{a}_{01}$	Undeformed Direction Vectors of Collagen Fibers
$\boldsymbol{a}_{02}$	Undeformed Direction Vectors of Collagen Fibers
c	The Stress-Like Parameter
$\bar{C}$	The Right Cauchy-Green Tensor
$\bar{I}_1$	The First Stretch Invariant
k_1	The Material Properties of Collagen Fibers
k_2	The Material Properties of Collagen Fibers

Chapter 1 - Introduction

1.1 Coronary Artery Diseases and Stent Treatment

Cardiovascular disease has been one of the deadliest diseases in the world and its incidence rate is increasing. According to the data provided by WHO, in 2016, around 17.9 million people died of this disease, accounting for approximate 30% of the total global deaths [1]. Especially, the coronary artery disease (CAD) associated with atherosclerosis accounts for the most of death. The plaques consisting of deposits of cholesterol and other lipids are formed in the inner surface of the coronary artery [2]. This pathological process is called atherosclerosis and it can cause the narrowing of arterial lumen, rupture of the arterial wall as well as hardening of the arteries, resulting in the reduction of blood flow [3]. There are multiple factors including high blood pressure, high cholesterol and poor diet which can lead to the formation of atherosclerosis. In the light of this, stent is a curial invention for the treatment of CAD.

Compared with bypass surgery, percutaneous coronary intervention (PCI) has been widely used in the treatment of CAD in recent years because of its minimal trauma, convenient operation and low risk. PCI Treatment usually treats CAD by implanting stents into patients. The stent is transported to lesion by a guide wire with catheter and expanded by the inflated balloon. The expanded stent is located at the lesion in order to increase the lumen diameter which can eventually restore the blood flow into normal condition. Although PCI is an effective treatment for CAD, the adverse events such as late in-stent restenosis (ISR) and stent thrombosis (ST) happening after a few years of stent implantation remain a major concern and are influencing long-term clinical outcomes. Hence, patients usually take medicine which could cause liver or kidney damage, such as aspirin, clopidogrel and ticagrelor to mitigate the formation of blood clots on stent. In order to alleviate ISR and ST, it is necessary to understand the causes and severity of them.

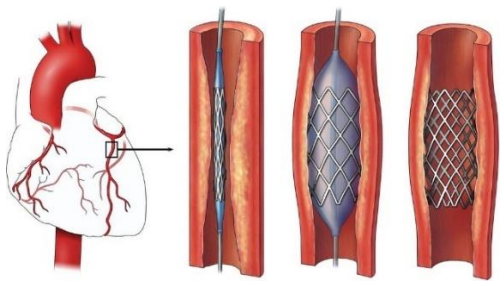

Figure 1. The Diagram of PCI Treatment with Stent Implantation [4]

1.2 Adverse Events of Stent Implantation and Stent Innovation

In-Stent Restenosis (ISR)

In-stent restenosis is defined as the re-narrowing of the segment of a treated coronary artery and it is still one of the main drawbacks of PCI treatment. The implanted stent will be wrapped by the growing blood tissue which could increase the difficulty of subsequent treatment. As reported by Pleva et al., the clinical incidence of ISR after the first-generation stent which is bare-metal stent (BMS) implantation is approximately 20%-35%. In order to mitigate this issue, the drug-eluting stent (DES) is designed and applied as second-generation stent which decreases the occurrence of ISR to 5%-10% [5]. Patient-specific factor and operational factor are two major aspects which can cause ISR. Patient-specific factor includes insufficient antiplatelet therapy and hypersensitivity reactions. Operational factor contains extensive tissue injury, stent malposition and stent dismantling [6].

Stent Thrombosis (ST)

Another adverse effect of PCI treatment is stent thrombosis which is defined as a thrombotic occlusion of a coronary stent. The use of DES to delay reendothelialization can effectively alleviate the issue of ISR, however it could also lead to the formation of ST [7]. Unlike the gradually process of ISR, ST usually leads to acute coronary syndromes with high mortality, such as cardiac death or myocardial infarction. As highlighted in Gori's study, the mortality of ST is around 5%-45% accounting for 20% of all myocardial infarction events after PCI treatment [8]. The patient factors involving diabetes, renal failure and stent factors involving impaired reendothelialization, stent malposition can induce ST.

1.3 Hemodynamics Analysis on Adverse Events

According to Koskinas' study, hemodynamic environment can negatively impact the formation of atherosclerosis. Additionally, a great number of studies suggest that wall shear stress-one metric of the hemodynamics may also contribute to the development of ISR and ST on the region where the plaque implanted with stent [6]. Therefore, the hemodynamics analysis including wall shear stress, time-averaged wall shear stress and oscillatory shear index needs to be conducted for the understanding of the development of ISR and ST. This could also contribute to the optimization of stents' and other cardiovascular devices' structure design aiming for a better hemodynamic performance.

Wall Shear Stress (WSS)

Wall shear stress is defined as the tangential stress derived from the friction of blood flow on the surface of inner vessel wall [9]. WSS can reflect the velocity distribution of the blood flow near the arterial wall. WSS has been confirmed that it has a critical relevance to the CAD with atherosclerosis. The region with low WSS is prone to form atheromatous plaque, while the area with high WSS may increase the risk of plaque rupture and thrombosis. A study from Beier et al. reported that the plaque which forms in the region with WSS < 0.5 Pa is more stable and stiffer [10]. In contrast, another study argued that although the area with WSS greater than 2.5 is not easy to form plaque, it will greatly promote the rupture of plaque and lead to vascular occlusion [11].

Time Averaged Wall Shear Stress (TAWSS)

Time averaged WSS is defined as the averaged value of the WSS during a cardiac cycle. The low TAWSS<0.5 Pa can cause cellular proliferation and intimal thickening [9]. These will finally result in the formation of ISR and ST.

1.4 Computational Fluid Dynamics (CFD) and Fluid Structure Interaction (FSI) for Hemodynamic Analysis

The implanted cardiovascular devices such as stents and heart valve prothesis require a long R&D cycle, many in-vitro experiment and multiple in-vivo clinical trials to ensure the optimized reliability, safety and biocompatibility. However, conducting in-vitro experiments needs expensive equipment and implementing in-vivo clinical trials is time-consuming. Computational fluid dynamics can numerically describe and evaluate the fluid flow of real-life problem. It has been widely used to analyze the hemodynamic objectives in coronary arteries and aortic valve with and without stent which are arduous to be measured in vivo. Compared with conducting in-vitro experiments and analyzing the data collected from patients, this method is more cost-effective and can provide relatively accurate results for cardiovascular device developers to design and optimize new devices and even for doctors to evaluate the condition of patients.

However, CFD has a significant disadvantage, that is, it cannot consider the deformation of tissues or organs due to blood flow when analyzing hemodynamic parameters. This is because CFD usually defines the fluid as a rigid wall. Hence, in order to alleviate this issue, a more advanced method called Fluid-Structure Interaction has been developed.

Fluid-structure interaction is a phenomenon that a solid structure deforms as a result of surrounding or internal fluid flow. In recent years, FSI approach has been utilized to a wide range of engineering systems including aerospace, automobile even biomedical.

One-way FSI and Two-way FSI are two FSI methods which have different characteristics. For one-way FSI, there is only data transmission from fluid domain to solid domain. In other words, the deformation of the solid domain will not in turn continue to affect the fluid domain. In Two-way FSI method, the governing equation of fluid and displacements of solid structure are resolved separately using two solvers. Therefore, there is data transmission between fluid domain and solid domain at the same time. The deformed model of solid domain will be transmitted to fluid domain for next computational step. Due to the data transmission between solid domain and fluid domain and the reconstruction of the mesh in fluid domain, the demand of computational power is massive. Additionally, another limitation of this method is instability. In conclusion, FSI simulation is an effective method for solving multi-physics problems. However, before conducting simulations for analyzing hemodynamics, it is significant to correctly define the actual problem. This is very helpful to select the correct simulation method. The workflow of two-way FSI simulation is shown in figure 2.

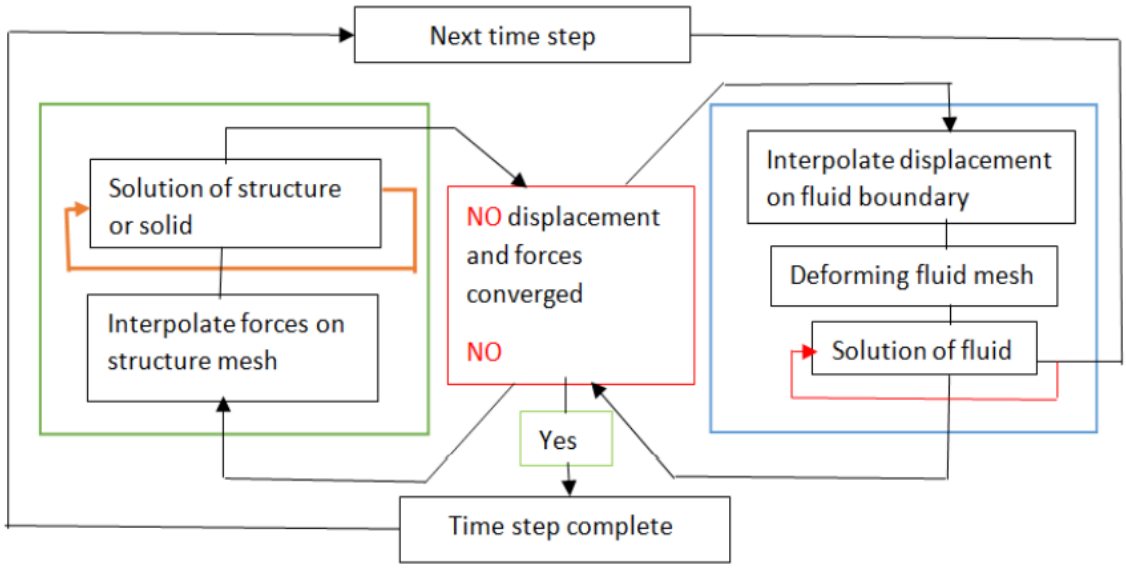

Figure 2. The Workflow of Two-Way FSI Method [12]

Chapter 2 - Literature Review

Chapter 2 provides a review of current literatures associated with the numerical modeling of a portion of coronary artery system. It contains the modelling of solid domain (coronary artery) and the modelling of fluid domain (blood).

2.1 Significance of FSI Simulation for Coronary Hemodynamic Analysis

As discussed in 1.3, the section of artery with low WSS and TAWSS is associated with the formation and growth of plaque and ISR. In contrast, the area with high WSS could cause plaque destabilization and plaque rupture. Hence, in order to acquire a better understanding of CAD, the study on hemodynamics and the quantification of hemodynamic metrics is significant. This can help the determination of the disease-prone artery and assist doctor to apply appropriate treatments for restoring normal blood circulation [13]. Moreover, this can also assist the R&D engineering of cardiovascular devices to design or optimize their products.

CFD is a valid method to quantify hemodynamic metrics without the use of expensive medical equipment. However, it can only be used to investigate pure blood flow problems. Since blood is pulsatile during the cardiac cycle, artery wall may deform. Due to this, if a stent is implanted in artery, the stent will also deform which could lead to the unstable hemodynamic environment. Therefore, for considering this phenomenon, it is crucial to apply FSI method to evaluate the mutual influence between blood and arterial wall. Current research on arterial problems using numerical simulation mainly use CFD method however, FSI method which is more realistic and accurate is rarely used. A study by Lopes et al. examined 49 articles of computational hemodynamic analysis and there were 36 articles which only used CFD to analyze the hemodynamics of coronary artery [13].

Although FSI method requires more computational power and more complex numerical modeling, it can provide more authentic evaluation of arterial hemodynamic problem. A study from Malvè et al. compared the computational results of hemodynamic metrics obtained from CFD and FSI method. They highlighted that the distribution of WSS and TAWSS were remarkably affected by the cardiac-induced vessel motion [14]. This means that for acquiring accurate hemodynamics objectives, the deformation of arterial wall cannot be neglected.

2.2 Solid Domain of FSI Simulation

In the numerical analysis of arterial hemodynamics using FSI method, solid domain controls

the mechanical behavior of arterial wall. Multiple studies have confirmed that the geometry and material definition of coronary artery are two major aspects which has significant influence on the accuracy of computational results.

The Geometry of Coronary Artery

In the numerical analysis of hemodynamics, the curvature of arterial wall and unsymmetrical structure are unique which leads to the difficulty of geometry modeling. Therefore, two methods are used by researchers to solve modeling problem, the idealized method and the patient-specific method.

The 3D arterial wall can be modelled by merging and stacking the 2D patient-specific image scans of MRI or CT [14]. In Siogkas et al.'s study, they performed a hemodynamic analysis on patient-specific model using FSI simulation. Firstly, the biplane angiographic data and intravascular ultrasound images were fused for reconstructing 3D geometry of artery. Then, the 3D intravascular ultrasound images catheter was reconstructed using the corresponding angiographic images. The 3D catheter path could guide the segmented frames in an appropriate direction. Finally, the nonuniform rational B-spline 3D surfaces were created using the two-point clouds representing the lumen and arterial wall [15]. This method usually costs a great amount of funding and needs to be approved by the relevant departments. Additionally, in order to obtain the valid and accurate computational results using CFD or FSI simulations, it is necessary to build appropriate mesh. However, the highly irregular surfaces usually could cause the generation of poor-quality mesh or even meshing failure. Therefore, there are relatively few studies using patient specific coronary artery bifurcation for hemodynamic analysis.

Figure 3. The 3D Patient Specific Reconstruction of The Coronary Artery [15]

As a simpler method, the idealization of coronary artery is widely used in most of the hemodynamic FSI studies. This method models the arterial wall as a cylinder with internal fluid domain and constant wall thickness [10,16,17 and 18]. The study performed by Chaichana et al. analyzed the the influence of coronary artery angle on hemodynamics based on patient-specific and idealized model. They demonstrated that the computational results of idealized and patient-specific model are consisted [19]. Furthermore, when studying the effect of stenosis severity on hemodynamics, the computational results are independent of the model used [20]. However, in the study of Kashyap et al., they evaluated the influence of arterial curvature on TAWSS and OSI using CFD and found that the hemodynamic computational results can be affected by the small variation of curvature and tortuosity [21]. An advantage of idealized method is that the idealized model allows stent and plaque to be easily constructed in it. This can help analyze the effects of plaque and stents on coronary hemodynamics. In light of this, the parameter of geometry should be considered more carefully in order to build a valid model.

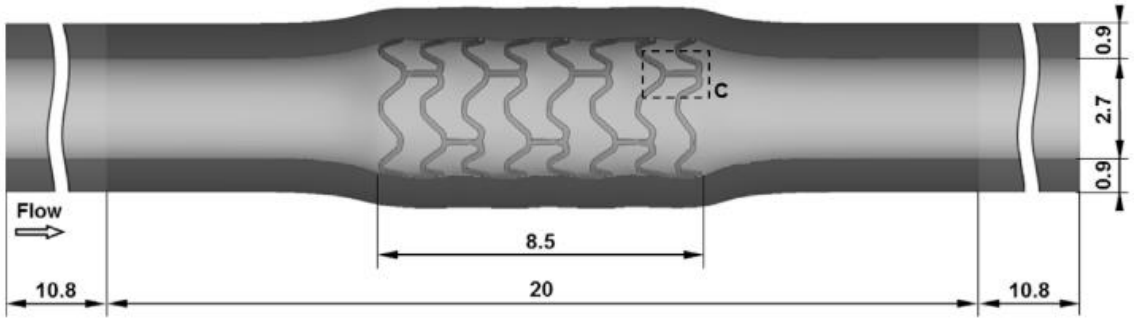

Figure 4. The Idelized Arterial Wall with Stent Implanted [18]

The Structure of Arterial Wall

The real arterial wall has three layers with different material properties. They are intima, media and adventitia. The three-layered model of arterial wall is illustrated in the figure below. The intima is the innermost layer of the arterial wall and the thinnest of the three layers. The long axis of endothelial cells is mostly consistent with the direction of blood flow, the nucleus is in the middle, the nucleus is slightly elevated, and the basal surface of cells is attached to the substrate. Tunica media is located between intima and adventitia. Its thickness and composition vary with the type of blood vessels. The aorta is mainly elastic membrane, with a few smooth muscles between them. Vascular smooth muscle fibers are thinner than visceral smooth muscle fibers and often have branches. The elastic fibers of the middle membrane can retract the dilated blood vessels, and the collagen fibers can maintain the tension and support the blood vessels. The study conducted by Gholipour et al. used the FSI simulation of idealized coronary artery

with one-layered and three-layered structure to predict the initiation of heart attack [22]. The results shows that the consideration of three-layered arterial wall structure has minimal effect on the hemodynamic parameters such as WSS. However, there is a significant difference on Von-Mises stress. This could result in the unrealistic simulation results. Hence it is significant to investigate if the three-layer arterial wall structure will affect the computational results of coronary bifurcation.

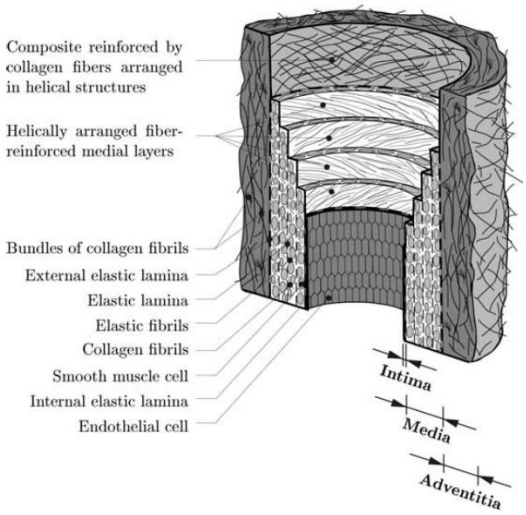

Figure 5. The Three-Layer Structure of Arterial Wall [23]

The Material Definition of Coronary Artery

The material properties of coronary artery can considerably affect the mechanical behavior which is caused by blood flow. If the material properties cannot be correctly defined, the interaction between arterial wall and blood cannot be authentically described. In addition, the simulation may fail due to the issue of element distortion caused by inappropriate material properties. In multiple studies, hyper-elastic material and linear-elastic material are used for defining arterial wall.

The material behavior of arterial wall is difficult to describe due to the non-homogeneous, anisotropic and stress-stiffening nature of the material [13]. Furthermore, the behaviors of arterial wall are usually nonlinear and hyper-elastic. Therefore, in most of the studies, the arterial wall was modelled as isotropic, homogeneous and incompressible hyper-elastic material. The stress-strain curve of this material is generated from the strain-energy function which is non-linear [14,18]. The most used hyper-elastic model is Mooney-Rivlin model. A study performed by Lee et al. used 5-parameter Mooney-Rivlin model to define the arterial wall and analyzed the mechanical behavior of stent and coronary artery due to the influence of

blood flow [17]. In Meza et al.'s study, they conducted the investigation of hemodynamics on left coronary artery and even considered the anisotropic properties into 5-parameter Mooney-Rivlin model which could influence the mechanical behavior of the arterial wall [24]. Although Mooney-Rivlin models with different parameters can provide more options for different working conditions, they still have limitations. Higher-order strain energy models can simulate more complex stress-strain curves. However, they also require more computational power, experiments, and parameter fitting. The computational results may be difficult to converge. Despite these limitations, the Mooney-Rivlin model can be considered as a sufficient material to model arterial wall.

Another straight-forward method is to define arterial wall as isotropic linear-elastic material. The material parameters are just Young's modulus and Poisson's ratio. Due to the development of hyper-elastic material, this method is hardly used in recent studies. A study from Kallekar et al. evaluated and compared the arterial wall flexibility using linear-elastic, Neo-Hookean and Mooney-Rivlin model. The results showed that the linear-elastic model overestimated the deformation of arterial wall [25]. Therefore, in order to obtain valid computational result, the linear-elastic model is not recommended.

The most complicated material model used for capturing the mechanical behavior of arterial wall is anisotropic hyperelastic model. The reason why arterial wall shows anisotropic behavior is because there are collagenous fibers inside the media and adventitia. Each of them is dispersed on different orientations. This finally leads to the different stiffness along the longitudinal and circumferential direction of arterial wall. When the soft tissue undergoes deformation, the elastin fibers cause the tissue to stiffen, storing the majority of the strain energy. The collagen fibers, meanwhile, are comparatively inextensible and loose. These fibers increase the tissue's stiffness when pulled tight, limiting the degree of deformation and protecting the tissue from injury. Because each of these collagen fiber families tend to have preferred directions, soft tissues possess anisotropic properties. This view was first confirmed by holzapfel through uniaxial tensile test of human arterial wall [23]. One of the most famous orthotropic hyperelastic model is called Holzapfel-Ogden-Gasser model. Holzapfel, Ogden and Gasser considered arterial wall as a composite panel containing matrix (smooth muscle cell, endothelial cell and elastin) and orthotropic reinforced fibers (collagenous fibers). The material model is demonstrated in figure 6. The study from Tricerri et al. conducted the FSI simulation for idealized cerebral arteries with isotropic and anisotropic material model. The results

indicate that the consideration of anisotropy has minimal impact on hemodynamics [26]. The variation between computational results using isotropic and anisotropic material model will be analyzed to identify the most appropriate material model for future simulation.

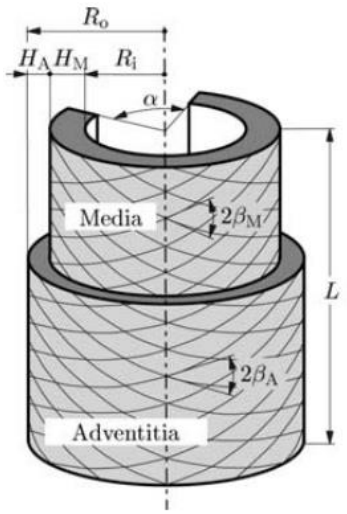

Figure 6. The HGO Orthotropic Hyperelastic Model Diagram [23]

2.3 Fluid Domain of FSI Simulation

In the numerical analysis of arterial hemodynamics using FSI method, fluid domain controls the fluid dynamic behavior of blood. For accurately describing the fluid characteristics and motion of blood, several aspects need to be considered and discussed in this section.

Inlet Blood Profile

Blood flow and blood pressure are unsteady and pulsatile during the cardiac cycle. This is the phenomenon of heart pump. Systole and diastole constitute a cardiac cycle which causes the variation of blood velocity. Hence, it is necessary to consider this phenomenon into the inlet blood velocity setting for conducting a realistic and valid simulation. Zeng et al. conducted a study on WSS of right coronary artery with both steady blood flow and pulsatile blood flow. The pulsatile blood flow was modelled using Womersley velocity profiles. They emphasized that the influence factor on WSS can be shifted by the inlet blood profile [27]. A study performed by Theodorakakos et al. analyzed the influence of pulsatile blood flow on coronary artery's fluid dynamics. They reported that compared with myocardial motion, the pulsatile blood flow can significantly affect the blood distribution in coronary artery [28]. Transient flowrate, Womersley velocity profile and transient pressure profile are widely used for modeling pulsatile blood flow. Appropriate and correct use one of these methods can make the computational results more valid, thus contributing to the numerical analysis of hemodynamics.

Outlet Pressure Profile

Outlet boundary condition has a significant effect when conducting the FSI simulation of coronary artery. This is because the deformation of arterial wall is mainly caused by the blood pressure. When the outlet is set to 0-gauge pressure, the blood pressure generated by the inlet blood flow can only reach to 100-500 Pa. In addition to this, if the outlet pressure is set to constant average blood pressure, the deformation of arterial wall will maintain in a steady state. Compared with the realistic range of blood pressure in human body, the computational results using these two boundary conditions could be inaccurate. However, due to the consideration of fluid boundary as the rigid wall in CFD simulation, 0-gauge pressure outlet will not affect the computational results. The influence of these different outlet boundary condition on the computational results will be evaluated in the stage one of this project.

Blood Characteristic and Viscosity Models

The hemodynamic simulation using Newtonian or non-Newtonian fluid to describe the blood has been critically debated by many researchers. Under the condition of large vessels, considering blood as the Newtonian fluid is widely accepted and can usually provide reasonable computational results. However, in the microcirculatory system and the artery with plaques, the assumption of Newtonian blood flow is inappropriate [20]. This is because the shear rates of different blood vessels are varying which can lead to the variation of blood viscosity. The region with a significantly low shear rate exhibits the clearest non-Newtonian behavior of blood. Multiple studies have highlighted that the non-Newtonian behavior of blood has a significant influence on the consistency between computational results and the data measured in vivo [29,30]. Amiri et al. analyzed hemodynamics for patient-specific femoral artery with a small plaque. The results showed that the substantial difference in the distribution of WSS and blood velocity was determined by whether the blood was considered as Newtonian or non-Newtonian [31]. Viscosity models has been investigated in many studies as a major factor that can affect the non-Newtonian behavior of blood. A study from Razavi et al. conducted a numerical simulation of pulsatile blood flow in a stenosed carotid artery using 6 non-Newtonian viscosity models. The computational results of WSS and velocity showed that the non-Newtonian behavior of blood was overstated by power-law model and the Walburn–Schneck model exhibited inapparent non-Newtonian behavior of blood. Additionally, the similarity among the modified-Casson, generalized power-law and Newtonian models are obvious. These two models underestimate the non-Newtonian behavior of blood. Different

from the first four models, the Carreau-Ysuda and Carreau models provided moderate global importance factor which is used to measure the non-Newtonian behavior [29]. Hence, these two models are most suitable for describing the non-Newtonian behavior of blood. This point of view has been confirmed by Kumar et al.'s study. They highlighted that the Carreau-Ysuda model provided better approximations for WSS and velocity distribution in the stenotic coronary artery [32].

Fluid Model

The blood flow in the healthy and large vessels can be considered as laminar. However, laminar to turbulent transition can occur due to the pulsatile nature of blood flow and the present of vascular lesions [33]. Multiple studies have considered this phenomenon into the numerical analysis of arterial hemodynamics and obtain valid computational results. Most of studies use k-ω or k-ω SST turbulence model to describe this phenomenon [34,35]. This is because k-ω model can provide more accurate results near the wall boundary for the problems which have wall boundary. The difference between them is that the k-ω SST model can describe the laminar to turbulent transition and can also provide accurate results both near and away the wall boundary. In the study of Ryval et al., they analyzed the pulsatile blood flow in stenosed vessels using both k-ω and k-ω SST models. Compared with the experimental data, the computational result showed that the steady and pulsatile blood flow could be appropriately described by k-ω SST model. The turbulence at and downstream of the plaque was overstated by the k-ω model [35]. Therefore, the k-ω SST model could be a valid model for the future FSI simulation.

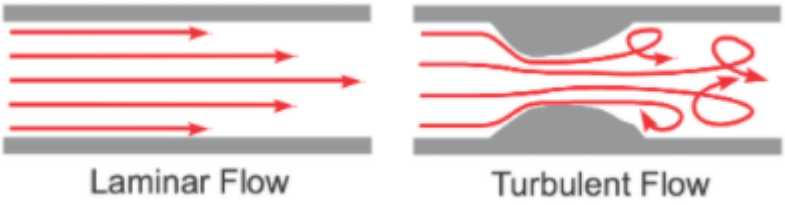

Figure 7. The Laminar to Turbulent Transition of Blood Flow [36]

Dynamic Mesh

When using FSI method to compute the interaction between arterial wall and blood domain, the fluid boundary is varying with the deformation of arterial wall simultaneously. This means that the mesh of blood domain will not remain the static state. If the dynamic mesh is not setup correctly, the issue of mesh distortion and negative mesh element may occur. These will finally lead to the breakdown of simulation. Hence, the implementation of appropriate dynamic mesh method in fluid domain is necessary. There are three kinds of dynamic meshing techniques

which are layering, smoothing and remeshing. Layering is the method which is often used for linear motion and the mesh type must be quadrilateral (2D) or hexahedron (3D). The basic principle of layering method is detecting the height of the mesh connected to the moving boundary and determining whether the mesh is split or merged by setting the height threshold. The remeshing method is that in the process of boundary movement, the program continuously detects the mesh quality in the computational domain and marks the low-quality mesh. In the process of dynamic mesh updating, the marked mesh is reconstructed. Smoothing is used to improve the quality of the mesh by adjusting the position of element nodes and it can only be used for triangular (2D) or tetrahedron (3D) mesh. This method is often used with remeshing at the same time [37].

2.5 Current FSI Simulation of Hemodynamics on Coronary Artery

Multiple studies have conducted FSI simulation for investigating hemodynamics of coronary artery with stent or with plaque. In the study from Zouggari et al., they implemented both CFD and FSI simulation for analyzing hemodynamics on the patient-specific coronary artery with the presence of plaque. The result showed that the low WSS area which could lead to the formation of atherosclerosis and inflammation and recirculation zone occur at the region after plaque. Compared with the results of FSI and CFD, there were considerable differences between blood velocity and WSS. They reported that the blood velocity was overestimated by CFD simulation due to the assumption of rigid arterial wall [38]. Furthermore, they highlighted that WSS was also overstated by CFD. This may mislead the assessment of the patient's condition. Similarly, a study from Lepos et al. compared the hemodynamic results of CFD and FSI. They also found that it is necessary to consider wall compliance during numerical simulation due to the overestimation of WSS and blood velocity profile using CFD [39].

2.6 Current FSI Simulation of Hemodynamics on Coronary Artery Bifurcation

The blood flow in the coronary artery trunk can be regarded as a parabolic lamina flow. However, under the condition of coronary artery bifurcation, the blood flow will become more complex. Compared with coronary artery trunk, the possibility of the formation of atherosclerosis around the bifurcation area is higher. In additional to this, with the consideration of arterial wall compliance using FSI method, there could be some unneglectable differences between the blood flow around bifurcation area computed using CFD method and FSI method.

Hence, the hemodynamic analysis of bifurcation is more significant and valuable. A study from Malvè et al. used FSI and CFD to simulate the coronary artery bifurcation. They found that the gap between minimal WSS calculated using FSI and CFD is around 50% [14]. This indicated that the deformation of arterial wall significantly influences the blood flow.

2.7 FSI Setup

After reviewing the literatures associated with FSI simulation of hemodynamics on coronary artery, a deeper understanding of FSI simulation setup has been achieved. The FSI setup of most studies are basically similar. In zouggari et al.'s study, they first used Magnetic Resonance Imagery (MRI) to reconstruct 3D patient-specific coronary artery as simulation geometry model. Then, a study of mesh quality was conducted for ensuring the computational accuracy. The transient inlet blood velocity profile was generated using 4D MRI images and the constant blood pressure was set as outlet boundary condition. The blood was assumed as non-Newtonian incompressible laminar flow with the Carreau viscosity model. The arterial wall was modelled using 5-parameter Mooney-Rivlin hyper-elastic model [38]. These setups and assumptions can make a great contribution to FSI simulation in the future.

2.8 Stent Structure

Although the focus of this study is not on the structure and design of stent, some literatures on this topic, have also been reviewed. This is to provide some ideas for the construction of stent geometric model. In the study of Beier et al., they conducted a simulation using idealized stent geometry to analyze stent parameters affecting coronary hemodynamics [10]. The result showed that the major cause of adverse wall shear stress gradient is the narrow strut spacing. Thinner struts have a positive influence on the blood flow leading to healthy WSS and they can help the recovery of blood flow. A study performed by Koskinas et al. analyzed the in vivo data and computational results of human coronary artery and investigated the relationship between WSS and the formation of ISR and ST. They highlighted that the in-stent region exposed to low WSS could be reduced by shorter connector length. Moreover, they also emphasized that oversized stent will not only increase the cross-sectional area of the blood vessel, moderate the blood velocity and cause low WSS to induce ISR, but may also damage the blood vessel and lead to ISR [6]. These provide assistances for future hemodynamic analysis and the selection of stent modeling parameters.

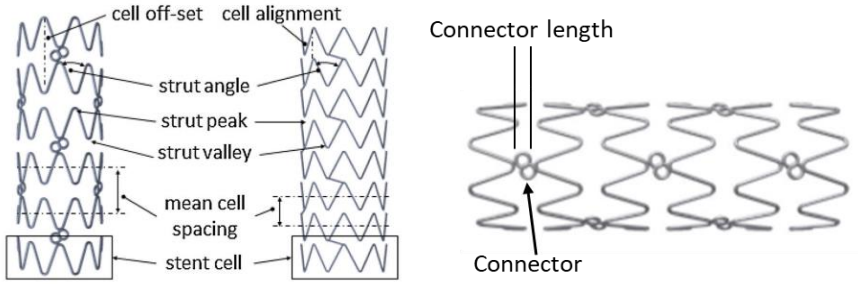

(a) **(b)**

Figure 8. (a) The Schematic of Stent Structure (b) The Schematic of Stent Connector [10]

2.9 Motivation for Research

FSI simulation has developed rapidly in recent years, and many recent hemodynamic simulation studies of coronary artery are based on FSI. However, a considerable number of studies are still using CFD to analyze it. Based on the reviewed literature, most of them use unrealistic assumptions such as Newtonian blood flow, linear elastic arterial, 0-gauge pressure outlet. Thus, there is a research gap in using realistic boundary conditions to define the numerical model of coronary artery. Therefore, the major motivation of this research is to build more accurate and realistic numerical model for analyzing hemodynamic parameters. Additionally, based on the literature, most of the studies perform FSI simulation on the coronary artery without the presence of stent. Therefore, there is a research gap in using two-way FSI simulation for evaluating the hemodynamics of coronary artery with stent. In addition to this, most of the previous studies assume the material of arterial wall as liner elastic or isotropic hyperelastic during the FSI simulation. This could impact the local hemodynamic results. Hence, consideration of arterial wall's anisotropic mechanical behiviour during the FSI simulation of stented coronary is a research gap. Hemodynamic analysis of stented and non-stented idealized coronary artery based on two-way FSI simulation with the consideration of arterial wall compliance will be conducted. The hemodynamic analysis patient specific coronary artery bifurcation with and without stent will also be conducted. The computational results using FSI of idealized coronary artery and patient specific coronary artery bifurcation will be compared with those using CFD to show the difference between FSI and CFD as well as the difference between hemodynamics of stented and non-stented coronary artery. By achieving these, the more realistic and accuracy numerical model can be defined. This can assist the R&D engineers of cardiovascular devices to optimize the hemodynamic performance of their products and even help doctor to quantify the situation of cardiovascular patients.

Chapter 3 – Methodology

3.1 Research Aims and Objectives

The aim of this study is to conduct both two-way FSI simulation and CFD simulation for analyzing hemodynamics of coronary artery under different geometry, material model, arterial wall structure and boundary conditions. The research objectives are to evaluate the influence of the arterial wall compliance on coronary hemodynamics metrics and compare these results with the results using CFD. Eventually, based on the evaluation, the more appropriate and accurate numerical model can be identified. This study is based on two-way FSI simulation which can accounts the interaction among stent, arterial wall and blood flow. The major hemodynamic metrics including blood velocity distribution, WSS and TAWSS will be determined and investigated.

The method used for analyzing research objective will be discussed in this section. Since the aim of this research is to build a realistic numerical model to analyze the hemodynamics of artery. A workflow diagram shown below illustrate the process of the whole thesis project.

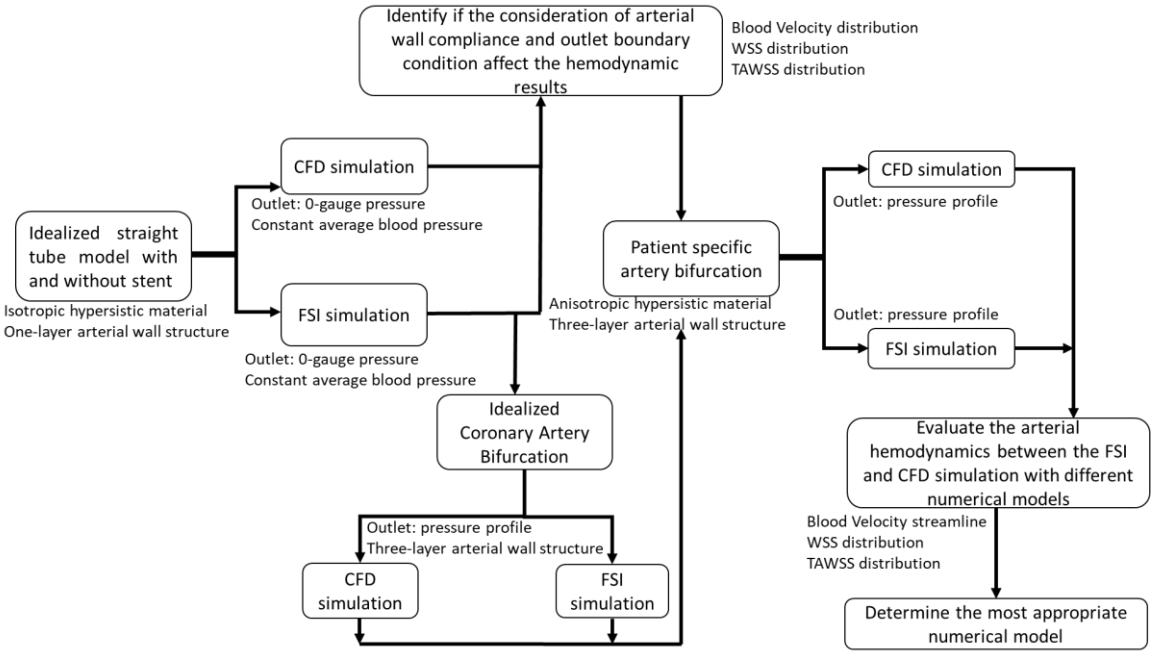

Figure 9. The Workflow of Research Thesis

The calculation time of FSI simulation is significantly long, and it is common for dozens of hours of simulation to be interrupted due to some issues. Additionally, there are many settings in the FSI simulation, which makes it difficult to conduct troubleshooting. Hence, some

idealized models need to be simulated first. These can not only build a foundation for the final realistic numerical model, but also obtain some useful results. The whole chapter will be divided into three parts. The first one and second one is the simulation setup of idealized coronary artery and bifurcation. The third one is the simulation setup of patient specific bifurcation.

3.2 Numerical Model of Idealized Coronary Artery with and without Stent

The Geometry Modelling of Idealized Arterial Wall and Stent

The idealized geometry model of stent and arterial wall was built in SolidWorks 2020. The stent is generated using the operation called ‘wrapping’ from a plane sketch. In real life, most of the stents are usually made by cutting stainless steel pipe or nitinol pipe with laser cutting machine. The path of laser cutting will be converted from plane sketch into G code by the software. The 3-D model and plane sketch are shown in figure 10 and 11. The dimensions of them are summarized in table 1 and 2. These dimensions and structure of stent are determined through literatures. In order to create the contact among stent, blood domain and arterial wall, they are pre-assembled in SolidWorks 2020 and then operated using Boolean operations in DesignModeler. The final geometry of stented idealized artery wall is shown in figure 12.

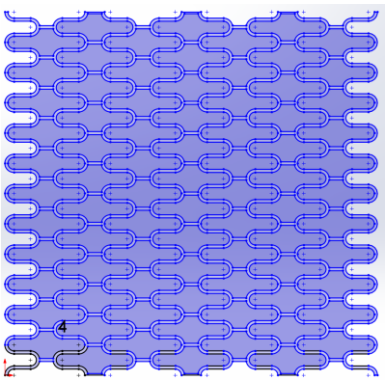

Figure 10. Plane Sketch of Stent

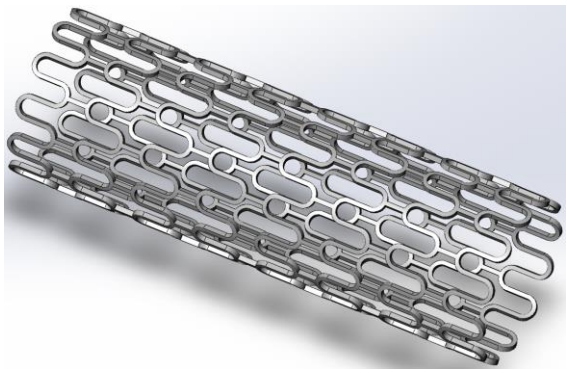

Figure 11. 3-D Geometry of Stent

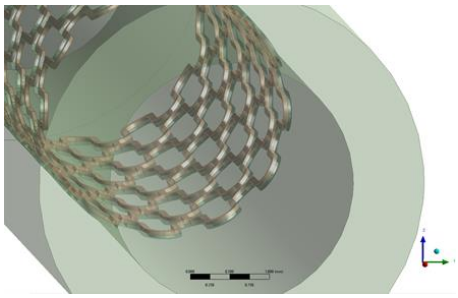

Figure 12. Idealized Coronary Artery with Stent

Table 1. The Dimensions of Idealized Arterial Wall

Properties	Dimension
The Length of Arterial Wall (mm)	35
The Thickness of Arterial Wall (mm)	0.9
The Diameter of Arterial Wall (mm)	3

Table 2. The Dimensions and Structure of Preliminary Stent

Properties	Dimension
Stent Diameter (mm)	3
Stent Length (mm)	9.7
Strut Diameter (μm)	100
Connector Length (mm)	0.36
Cell Height (mm)	2
Number of Cells	12
Number of Connectors	12
Number of Peaks	12
Alignment Type	Peak-to-Peak
Connector Structure	Straight
Strut Cross-Sectional Shape	Rectangular

Numerical Modelling of Solid Domain

The Transient Structural modulus in ANSYS 21.1 will be used for simulating the mechanical behavior of the stent and arterial wall. Due to the unsteady nature of pulsatile blood flow, the transient analysis is more appropriate in this situation. It can capture the mechanical behavior of stent and arterial wall at each timestep. The boundary condition in solid domain is the fixed support at the inlet and outlet cross-sectional surfaces of arterial wall. This is for avoiding the rigid body motion. Another one is the solid-fluid interface at the inner surface of the arterial wall and the contact surface between stent and blood. This is the place where the fluid domain and the solid domain interact their data. The contact between stent and the inner surface of arterial wall is set to be bonded. This is a correct assumption because when the stent is implanted into the human body, there is almost no longitudinal displacement. The boundary

conditions are shown in figure 13.

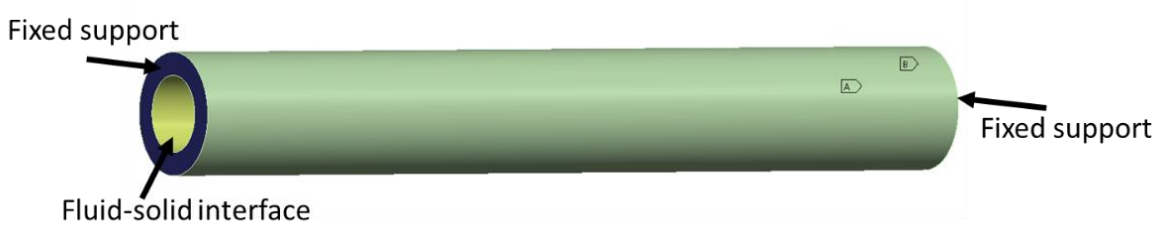

Figure 13. The Boundary Conditions of Solid Domain (Idealized Coronary Artery with Stent)

The material used for simulating the mechanical behavior of stent is Nitinol which is widely used for manufacturing stent due to its outstanding biocompatibility and mechanical properties. In this project, the Nitinol is assumed as the linear-elastic material. The material used for simulating the mechanical behavior of idealized coronary is hyper-elastic material called 5-parameter Moony-Rivlin. It has been discussed in previous section. The time step is set to 0.024 s. the step end time is set as 0.72 s representing one cardiac cycle. Due to the exponentially increasing computational time of FSI simulation, the hemodynamic analysis is only conducted in one cardiac cycle. The von-Mises stress and total deformation of stent and arterial wall will be analyzed for evaluating their influences on local hemodynamics. The material properties of stent and arterial wall are summarized in table 3 and 4. The strain energy equations of incompressible 5-parameter Mooney-Rivlin model are given below [17].

$$W = C_{10}(\overline{I_1} - 3) + C_{01}(\overline{I_2} - 3) + C_{20}(\overline{I_1} - 3)^2 + C_{11}(\overline{I_1} - 3)(\overline{I_2} - 3) + C_{02}(\overline{I_2} - 3)^2 + \frac{1}{D_1}(J - 1)^2 \quad (4)$$

$$D_1 = \frac{1 - 2\nu}{C_{10} - C_{01}} \quad (5)$$

$$\overline{I_1} = {\lambda_1}^2 + {\lambda_2}^2 + {\lambda_3}^2 \quad (6)$$

$$\overline{I_2} = {\lambda_1}^2{\lambda_2}^2 + {\lambda_2}^2{\lambda_3}^2 + {\lambda_1}^2{\lambda_3}^2 \quad (7)$$

$$\overline{I_3} = {\lambda_1}^2{\lambda_2}^2{\lambda_3}^2 \quad (8)$$

Where W is the strain-energy potential, $\overline{I_1}$ and $\overline{I_2}$ are the stain invariants, D_1 is the incompressible parameter, ν is Poisson's ratio, λ_1, λ_2 and λ_3 are the principal stretches and C_{10}, C_{01}, C_{20}, C_{11} and C_{02} are the Mooney-Rivlin coefficients.

Table 3. The Material Properties of Stent [40]

	Young's Modulus (GPa)	Poisson's Ratio	Yield Stress (MPa)	Ultimate Stress (MPa)	Density (kg/m^3)
Nitinol	79	0.33	443	1400	6450

Table 4. The Properties of 5-Parameter Mooney-Rivlin Model [17]

	C_{10} (MPa)	C_{01} (MPa)	C_{20} (MPa)	C_{11} (MPa)	C_{02} (MPa)	D_1 (MPa^{-1})	Density (kg/m^3)
Arterial Wall	-8.418	9.189	70.101	-185.38	128.346	0.012	1366

Due to the small surfaces introduced by the present of stent, the current mesh is unstructured tetrahedron mesh with the denser mesh around the area where the stent exists. The mesh of idealized coronary artery with stent is shown in figure 14.

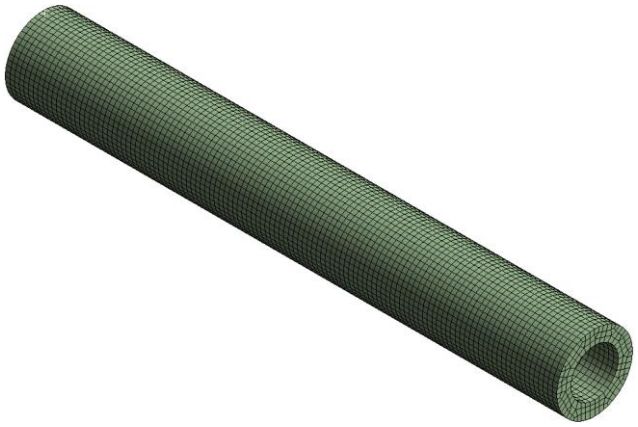

Figure 14. The Mesh of Solid Domain

Numerical Modelling of Fluid Domain

The FLUENT modulus in ANSYS 21.1 will be used for simulating the hemodynamic behavior of idealized coronary artery with and without stent. The hemodynamics during cardiac cycle is not a steady state condition, therefore, transient simulation will be used in the whole project. In order to ensure that the blood flow will fully develop, the extra length should be generated before the inlet and after the outlet. The equation used for calculating that length is given below.

$$Extra\ length = 0.06 \times Re \times stent\ diameter \quad (9)$$

Where *Re* is the Reynolds number of blood flow

Referring to section 2.3, the inlet boundary condition is set as pulsatile blood flow with

parabolic velocity profile. The parabolic blood profile is caused by the boundary layer theory. Due to the greater viscous force near the boundary layer, the velocity of the fluid near the boundary layer is slower than that of the center. The inlet velocity waveform assuming heartbeat as 75 beats/min is used from Nichol et al. (figure 15) [41]. The equation used for describing this flow is given below. In FLUENT, the inlet boundary condition is defined using user defined expression with the transient velocity table created by Ramtin (figure 16).

$$V_{Inlet} = V_{Max}\left[1 - \left(\frac{r}{R}\right)^2\right] \tag{10}$$

Where V_{Inlet} is the parabolic inlet profile, V_{Max} is the velocity at centerline, r is the distance between origin and an arbitrary point and R is the diameter of coronary artery.

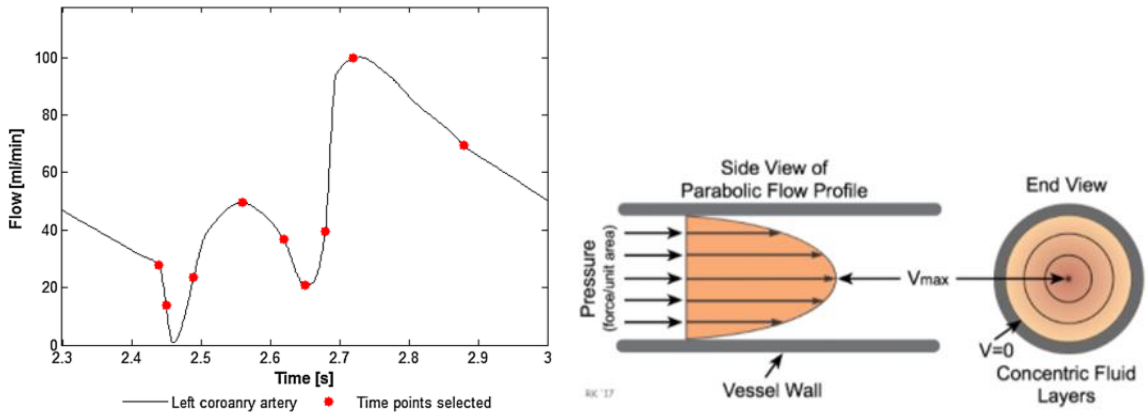

(a) **(b)**

Figure 15. (a) The Waveform of Pulsatile Blood Velocity [41] (b) Parabolic Velocity Distribution in Blood Vessel [42]

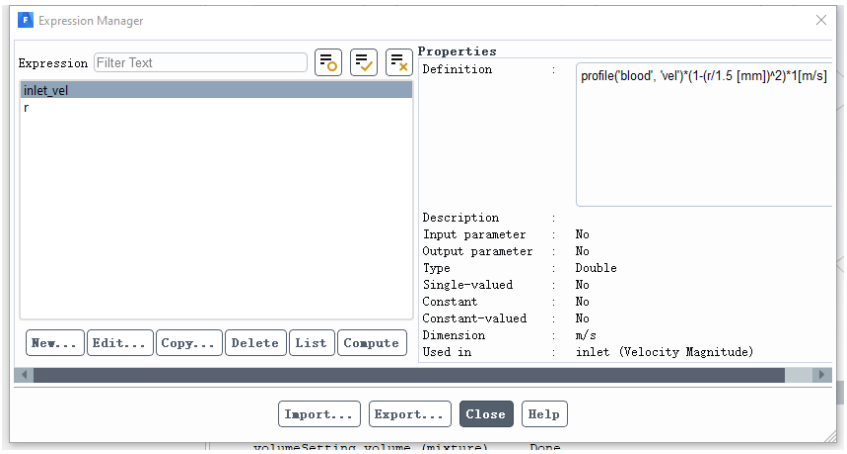

Figure 16. The User Defined Expression of Inlet Blood Velocity Profile

The outlet boundary condition is set to be constant static pressure with the value of 10400 Pa which is the average blood pressure of healthy human. The time step and end time are same as

solid domain which are 0.024 s and 0.72 s, respectively. The mesh of fluid domain is tetrahedron with inflation layers. The inflation layers are used for ensuring the smooth transient of mesh between the boundary wall and internal region. The residual target used in current simulation for ensuring computational convergence is 0.001. The density of blood is assumed to be 1060 kg/m^3 [18]. Blood is assumed to be non-Newtonian fluid and the viscosity model used for describing the non-Newtonian behavior of blood is Carreau-Ysuda model. The equation of Carreau-Ysuda viscosity model is given below [43].

$$\mu = \mu_\infty + (\mu_0 - \mu_\infty)[1 + (\lambda\dot{\gamma})^q]^{\frac{n-1}{q}} \quad (11)$$

Where μ is the variation of viscosity, μ_∞ is infinite-shear viscosity, μ_0 is zero-shear viscosity, λ is the time constant, $\dot{\gamma}$ is the shear strain rate, q is the Yasuda exponent, n is power index.

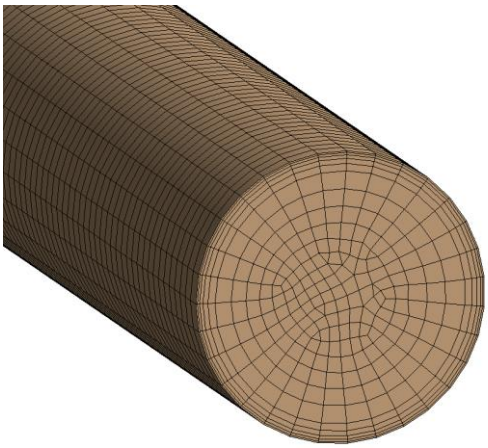

Figure 17. The Mesh of Fluid Domain

The computational results can be significantly influenced by mesh quality and mesh type. Hence, it is necessary to conduct mesh sensitivity study for ensuring the accuracy of computational results. The mesh quality is basically controlled by orthogonal quality (0.2-1) and skewness (0-0.8). The smaller the skewness, the better the mesh quality, and the larger the orthogonal quality, the better the mesh quality. The shape of the mesh is related to its computational convergence ability. For example, the convergence ability of a hexahedron mesh is stronger than that of a tetrahedron mesh. However, it is hard to generate hexahedron by slicing the complex geometry. The size of mesh determines the computational accuracy and time. An appropriate mesh size can reduce the demand of computational power while ensuring the convergence of the results. In the simulations of idealized coronary artery, the element size is set to 0.3 mm.

Table 5. The Parameter of Mesh

Element Size (mm)	Number of Elements	Average Skewness	Average Orthogonal Quality
0.3	54150	0.102	0.988
0.2	119700	0.0946	0.988
0.1	726250	0.0745	0.989

In order to obtain the result of TAWSS several operations need to be set in FLUENT. The operation of time statistics should be selected for letting FLUENT to compute time-averaged parameters during a period. In the calculation activities

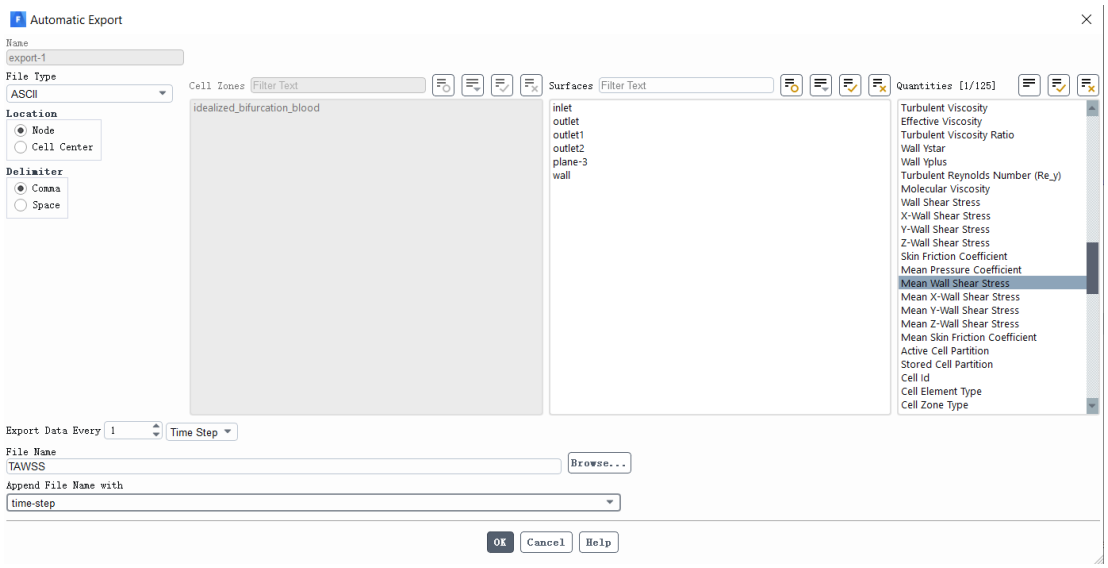

Figure 18. The Computational Setting of TAWSS in FLUENT

The dynamic mesh setting is important to maintain the quality of the mesh when the fluid domain deforms with the arterial motion. According to section 2.4, smoothing and remeshing are used in the whole project. This is because the mesh generated in all the numerical models are tetrahedron and the motion of blood domain is not linear. Hence, layering cannot be used in this condition. In addition to this, the arterial wall deformation caused by blood flow is small. Therefore, it is helpful to improve the quality of reconstructed mesh.

Another significant setting which has influence on the accuracy of computational results is discretization scheme in FLUENT. The ‘Coupled’ scheme is selected for conducting FSI simulation. This is because the time step used for FSI simulation is relatively large and the mesh size is larger than that in CFD simulations. Hence, for ensuring the computational accuracy, using this scheme is necessary. The transient formulation is set as ‘Second Order

Implicit' aiming for improving the accuracy during the transient simulation.

Setup of Two-Way FSI Simulation

System coupling is used to establish the interaction between fluid domain and solid domain. The workflow is shown in figure 19. The analysis setting in this modulus is set time step and end time as same as those in fluid and solid domain. The interaction is achieved by setting data transfer between fluid wall and fluid solid interface. The Maximum iterations is set to 10 to obtain converged results. These setups are shown in figure 20.

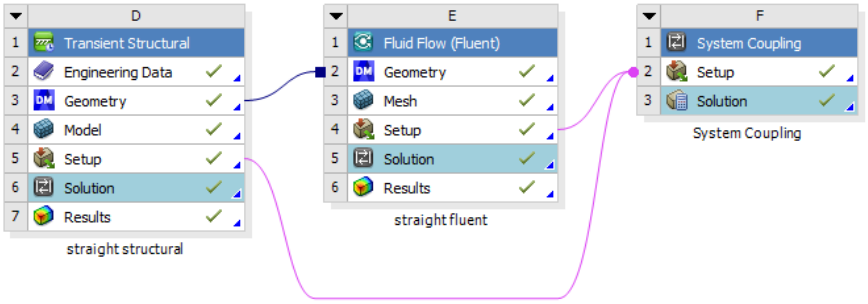

Figure 19. The Workflow of Two-Way FSI Simulation

Properties of Analysis Settings

	A	B
1	Property	Value
2	Analysis Type	Transient
3	Initialization Controls	
4	Coupling Initialization	Program Controlled
5	Duration Controls	
6	Duration Defined By	End Time
7	End Time [s]	0.72
8	Step Controls	
9	Step Size [s]	0.024
10	Minimum Iterations	1
11	Maximum Iterations	5

Figure 20. The Analysis Settings of Two-Way FSI Simulation

3.3 Numerical Model of Idealized Coronary Artery Bifurcation with and without Stent

The situation of hemodynamics at the bifurcation is much more complicated than that of the coronary artery trunk. Therefore, it is valuable to consider the arterial wall compliance using FSI to see if FSI can provide more realistic results.

The Geometry Modelling of Idealized Arterial Wall and Stent

The idealized coronary bifurcation is modelled through SolidWorks. Similarly, the contact regions among stent, blood domain and arterial wall are created using the Boolean operation in ANSYS DesignModeler. The geometries are shown in figure 21 below. The dimension of

idealized bifurcation is shown in figure below. The three-layered arterial wall structure is consternated using the Shell operation in SolidWorks 2020 and modified in ANSYS DesignModeler.

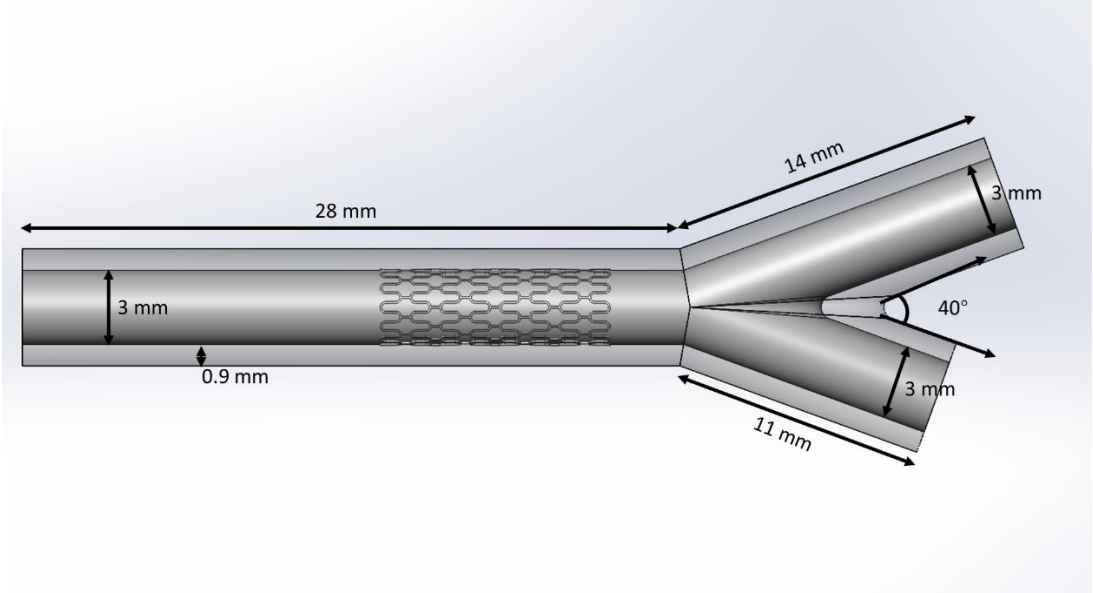

Figure 21. The Dimension of Idealized One-Layered Coronary Artery Bifurcation with Stent

Numerical Modelling of Solid Domain

Similar to the settings of previous simulation. The inlet surface and two outlet surfaces are set as the fixed support. The fluid-solid interfaces are the inner surface of arterial wall and the surface of stent contacting with blood domain. The contact between stent and inner surface of arterial wall is set as bonded. However, due to the implementation of three-layered arterial wall structure, the contact among intima, media and adventitia must be defined correctly. As a medium, the elastic membrane connects the inner membrane and the media, and the outer membrane and the media. Hence, the bonded contact is suitable in this condition. The overall mesh size of the whole arterial wall and blood domain are set as 0.3 mm. The mesh size at the contact region among stent, arterial wall and blood domain are set as 0.1 mm. The material model used for describing the non-linear mechanical behavior is isotropic 5 parameter Mooney-Rivlin hyperelastic model.

Numerical Modelling of Fluid Domain

The inlet blood profile is identical as the previous simulation. Fluid model is k-omega SST, the discretization scheme is set as coupled and the transient formulation is set as second order upwind. The dynamic mesh setting is same as previous simulations and activated on the wall where the data is transmitted.

According to the computational results of idealized coronary artery in 4.1, the 0 gauge-pressure outlet should not be used in FSI simulation. What is more, the blood pressure is varying with time, thus the constant 13332 Pa (100 mmHg) pressure outlet is also insufficient. In order to optimize the numerical model in fluid domain. A pulsatile outlet pressure profile which can matched with the inlet blood flow profile needs to be applied for next FSI simulation. The outlet pressure profile is show in figure 22 below.

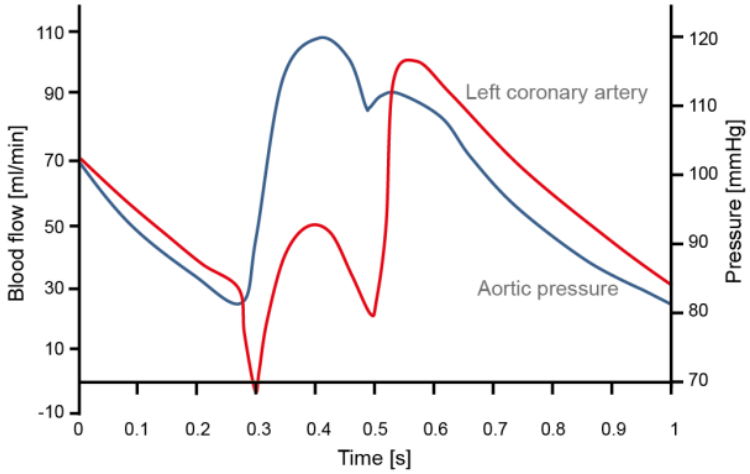

Figure 22. The Pulsatile Blood Flow and Pressure Profile During One Cardiac Cycle [41]

The pressure data is obtained using the software called WebPlotDigitizer-4.5. Each data point can be acquired through the automatic extraction by setting up the color of the curve. The sampling time step and the total time should be modified to be same as those used in the first stage FSI and CFD simulation.

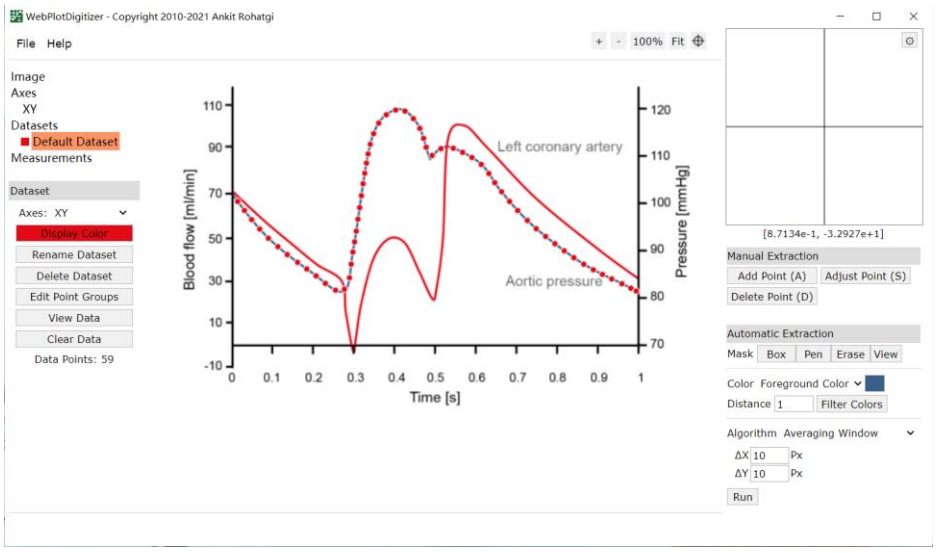

Figure 23. The Operation for Obtaining Data Points of Outlet Blood Pressure Profile

3.4 Numerical Model of Patient Specific Coronary Artery Bifurcation with and without Stent

Based on the experience of previous simulations, the final stage of the whole project will implement the three-layered arterial wall structure and anisotropic hyperelastic material for patient specific bifurcation to finalize the most appropriate and accurate numerical model.

The Geometry Modelling of Patient Specific Coronary Artery Bifurcation

The geometry of blood domain of patient specific coronary artery bifurcation is sent by Susann. By using the repair function in SpaceClaim, the deficiencies in the geometric model such as snitches, small surfaces are fixed. The arterial wall is built in SolidWorks 2020 using the Shell operation and modified in ANSYS DesignModeler using Boolean operation. Due to the irregular geometry of patient specific geometry, the stent is modelled along the centerline of the patient specific geometry ring by ring in SolidWorks 2020. The contact region among stent, blood domain and arterial wall is created in ANSYS DesignModeler. The three-layered patient specific bifurcation without stent and the one-layered patient specific bifurcation with stent is shown in figure 24 and 25 below.

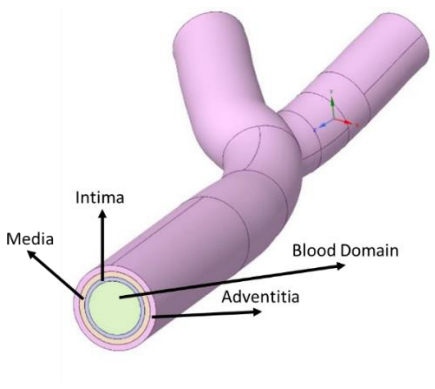

Figure 24. The Geometry of Patient Specific Three-Layered Coronary Artery Bifurcation without Stent

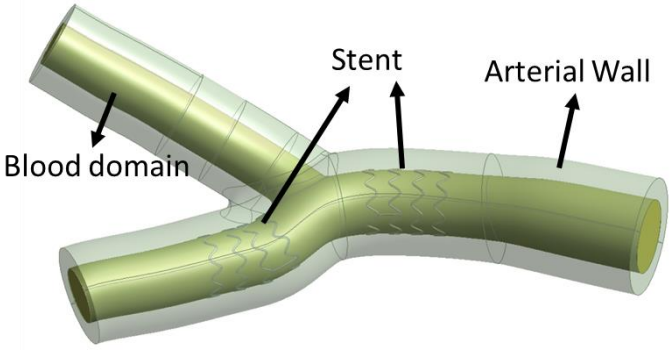

Figure 25. The Geometry of Patient Specific One-Layered Coronary Artery Bifurcation with Stent

Numerical Modelling of Solid Domain

The boundary conditions are almost identical to the second stage simulations. The anisotropic hyperelastic material will be introduced and defined in this section.

As discussed in 2.2, the anisotropic behavior of arterial wall is mainly caused by the collagen fibers helically existing in media, adventitia. There are no fibers in intima, thus intima can be considered as isotropic hyperelastic material. Media and adventitia can be regarded as fiber reinforced composite which has two collagen fiber families [22]. In Holzapfel et al.'s study, each layer is assumed to have same mechanical properties. Hence, the strain-energy equation of each layer will have the same form. This equation can be divided into two parts which are isotropic and anisotropic part. Isotropic part can describe the mechanical behavior of hyperelastic matrix which is the combination of tissue and endothelial cell. Anisotropic part can describe the mechanical behavior of collagen fibers. This equation is given below.

$$\bar{\Psi}(\bar{\boldsymbol{C}}, \boldsymbol{a}_{01}, \boldsymbol{a}_{02}) = \bar{\Psi}_{iso}(\bar{\boldsymbol{C}}) + \bar{\Psi}_{aniso}(\bar{\boldsymbol{C}}, \boldsymbol{a}_{01}, \boldsymbol{a}_{02}) \tag{11}$$

Where $\bar{C}$ is the right Cauchy-Green tensor, $\boldsymbol{a}_{01}$ and $\boldsymbol{a}_{02}$ are the undeformed direction vectors of collagen fibers.

The isotropic part can be treated using the neo-Hookean hyperelastic material model.

$$\bar{\Psi}_{iso}(\bar{\boldsymbol{C}}) = \bar{\Psi}_{iso}(\bar{I}_1) = \frac{c}{2}(I_1 - 3) \tag{12}$$

Where $\bar{I}_1$ is the first stretch invariant, c is the stress-like parameter.

Two invariants $\bar{I}_4$ and $\bar{I}_6$ are introduced to represent the square of the stretch along the direction of two collagen fibers. Under the higher loading condition, the stiffness of each arterial layer shows an exponential increase. This is purely caused by collagen fibers. Hence an exponential function is used to describe the strain energy equation.

$$\bar{\Psi}_{aniso}(\bar{\boldsymbol{C}}, \boldsymbol{a}_{01}, \boldsymbol{a}_{02}) = \frac{k_1}{2k_2}\{exp[k_2(I_4 - 1)^2] - 1\} + \frac{k_1}{2k_2}\{exp[k_2(I_6 - 1)^2] - 1\} \tag{13}$$

Where k_1 and k_2 are the material properties of collagen fibers,

Based on the equations above, the final strain energy potential equation using for describing anisotropic hyperelastic behavior of three-layered arterial wall is defined as:

$$\bar{\Psi}(\bar{I}_1, \bar{I}_4, \bar{I}_6) = \frac{c}{2}(I_1 - 3) + \frac{k_1}{2k_2}\sum_{i=4,6}\{exp[k_2(I_i - 1)^2] - 1\} \quad (14)$$

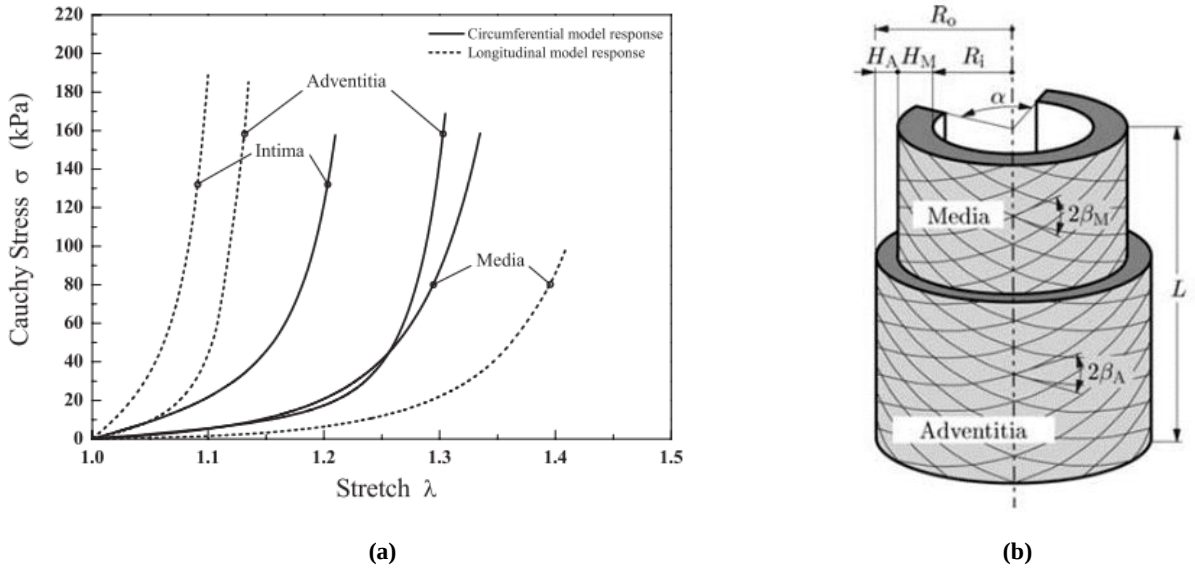

(a) **(b)**

Figure 26. (a) The Stress-Strain Plot of Different Layers Obtaining Through Uniaxial Tension Test; (b) The Anisotropic Hyperelastic Material Model Created by Holzapfel et al. [23]

In order to calibrate the anisotropic hyperelastic material properties from the given data in Holzapfel's literature and generate the APDL code in ANSYS, the software called Mcalibration is used. Firstly, the data points of stress-strain plot are obtained using WebPlotDigitizer-4.5 and then inserted into Mcalibration. The angles of two collagen fibers are 29° and 62° [23]. Hence, cos 14.5° and sin 14.5° are used to represent the direction vector of the first fiber. Similarly, the direction vector of second fiber can also be defined as cos 31° and sin 31°. It should be noted that the direction vectors in the code are based on the cylindrical coordinate system. The calibrated stress-strain plots and the APDL code of anisotropic hyperelastic material are shown below.

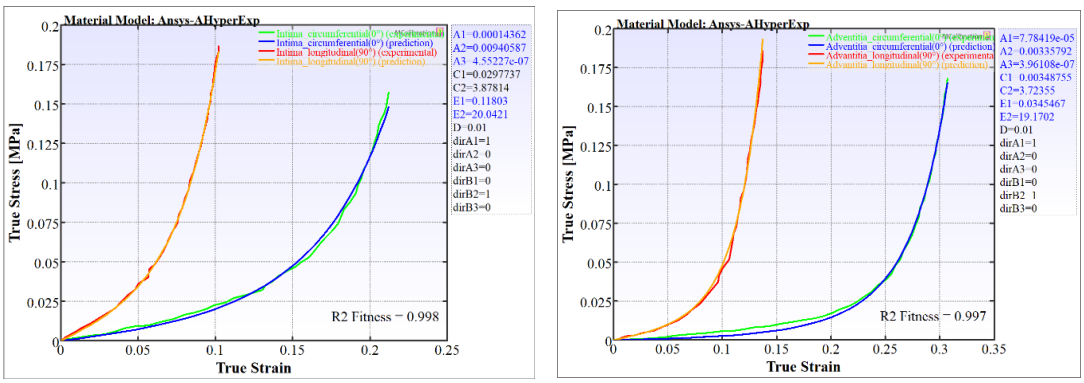

Figure 27. The Calibration of Orthotropic Material Properties of Adventitia and Intima

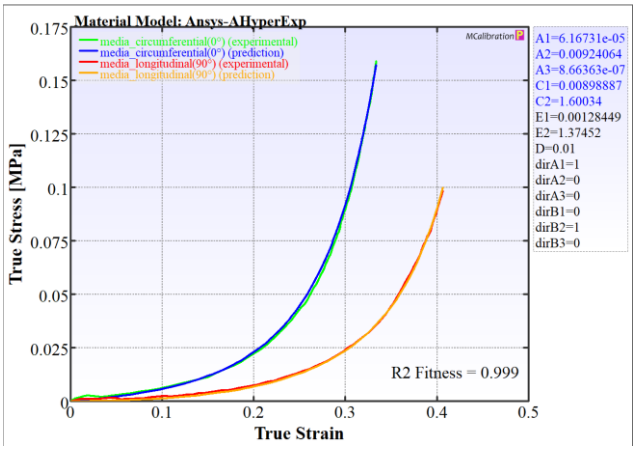

Figure 28. The Calibration of Orthotropic Material Properties of Media

```
TB, AHYPER, matid, 1, 10, EXP
TBDATA,  1, 10.43620361623 ! A1
TBDATA,  2, 0.00940587319029 ! A2
TBDATA,  3, 4.55227174045 ! A3
TBDATA,  4, 0.0 ! B1
TBDATA,  5, 0.0 ! B2
TBDATA,  6, 0.0 ! B3
TBDATA,  7, 0.0297736522126 ! C1
TBDATA,  8, 3.87813725865 ! C2
TBDATA,  9, 0.118030100182 ! E1
TBDATA, 10, 20.0421428063 ! E2

TB, AHYPER, matid, 1, 1, PVOL
TBDATA, 1, 0.01 ! D

TB, AHYPER, matid, 1, 3, AVEC
TBDATA, 1, 0
TBDATA, 2, cos(49.98)
TBDATA, 3, sin(49.98)

TB, AHYPER, matid, 1, 3, BVEC
TBDATA, 1, 0
TBDATA, 2, cos(-49.98)
TBDATA, 3, sin(-49.98)
MP, DENS, matid, 1.366e-09
```

(a)

```
TB, AHYPER, matid, 1, 10, EXP
TBDATA,  1, 6.16730705637 ! A1
TBDATA,  2, 0.00924064248682 ! A2
TBDATA,  3, 8.66363298257 ! A3
TBDATA,  4, 0.0 ! B1
TBDATA,  5, 0.0 ! B2
TBDATA,  6, 0.0 ! B3
TBDATA,  7, 0.00898887198008 ! C1
TBDATA,  8, 1.60033854323 ! C2
TBDATA,  9, 0.00128448623239 ! E1
TBDATA, 10, 1.37451594375 ! E2

TB, AHYPER, matid, 1, 1, PVOL
TBDATA, 1, 0.01 ! D

TB, AHYPER, matid, 1, 3, AVEC
TBDATA, 1, 0
TBDATA, 2, cos(49.98)
TBDATA, 3, sin(49.98)

TB, AHYPER, matid, 1, 3, BVEC
TBDATA, 1, 0
TBDATA, 2, cos(-49.98)
TBDATA, 3, sin(-49.98)
MP. DENS. matid. 1.366e-09
```

(b)

```
TB, AHYPER, matid, 1, 10, EXP
TBDATA,  1, 7.78418608675 ! A1
TBDATA,  2, 0.00335791737492 ! A2
TBDATA,  3, 3.96108001596 ! A3
TBDATA,  4, 0.0 ! B1
TBDATA,  5, 0.0 ! B2
TBDATA,  6, 0.0 ! B3
TBDATA,  7, 0.0034875488039 ! C1
TBDATA,  8, 3.72355405029 ! C2
TBDATA,  9, 0.0345466874437 ! E1
TBDATA, 10, 19.1701756153 ! E2

TB, AHYPER, matid, 1, 1, PVOL
TBDATA, 1, 0.01 ! D

TB, AHYPER, matid, 1, 3, AVEC
TBDATA, 1, 0
TBDATA, 2, cos(49.98)
TBDATA, 3, sin(49.98)

TB, AHYPER, matid, 1, 3, BVEC
TBDATA, 1, 0
TBDATA, 2, cos(-49.98)
TBDATA, 3, sin(-49.98)
MP, DENS, matid, 1.366e-09
```

(c)

Figure 29. The ANSYS APDL code of Anisotropic Hyperelastic Material Model: (a) Intima; (b) Media; (c) Adventitia

In order to use this material model, correctly defining coordinate system is significant. One local cylindrical coordinate system at the center of gravity of the geometry is sufficient for the transformation of the material properties in the global cartesian coordinate into local coordinate cylindrical system. Despite this, if the geometry is an idealized coronary artery bifurcation, the whole geometry can need to be divided into three parts. There will be three local cylindrical coordinate systems to define the material properties for each part.

Numerical Modelling of Fluid Domain

The inlet is set as parabolic pulsatile blood profile and two outlets are set to the pulsatile blood pressure in the second stage simulations. the rest of settings are identical to second stage simulations.

Chapter 4 - Results

4.1 The Results of Stented and Non-Stented Idealized Coronary Artery

In order to build the foundation for the more complex simulation using idealized and patient specific coronary bifurcation. Eight simulations have been conducted using the idealized coronary artery and stent with different outlet boundary conditions. The results of them are shown below.

To validate the inlet parabolic blood profile, the contour plot of velocity distribution using FSI method at 0.72 s are given below. It can be concluded that the parabolic velocity distribution can match with the inlet blood flow setting. In another contour plot, the blood flow pulse appears on the left. This can confirm the successful construction of the pulsatile blood flow boundary conditions.

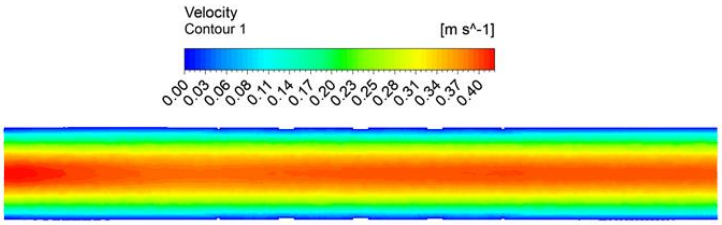

Figure 30. The Parabolic Blood Profile

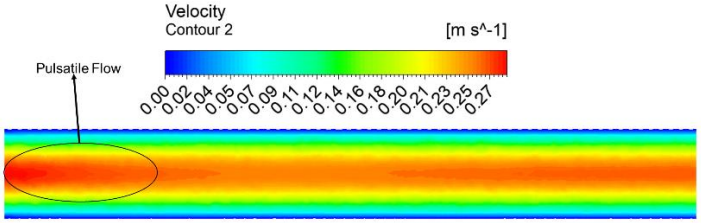

Figure 31. The Pulsatile Blood at One Time Step

In order to figure out if there is the difference between the hemodynamic results using FSI method and that using CFD method, the line chart of WSS distribution at each time step and the velocity distribution at each time step are shown in figure below. The results in line chart are computed using constant 13332 Pa (100 mmHg) outlet pressure. It can be seen that the WSS computed using FSI and the WSS computed using CFD are almost identical. However, the WSS of CFD at 0.524 s is slightly higher than that of FSI. Before 0.524 seconds, the arterial wall in FSI simulation can be regarded as a rigid wall because the pressure generated by blood flow velocity can hardly deform the arterial wall. Hence, with the same velocity, radius and

viscosity, the WSS of FSI and CFD are identical. However, at 0.524 s the blood pressure generated by the peak blood velocity causes the radial expansion of the arterial wall. Additionally, the blood flow radius remains constant in the CFD simulation. Therefore, when the viscosity and speed remain unchanged, and the radius becomes larger, the WSS of FSI will be lower than that of CFD.

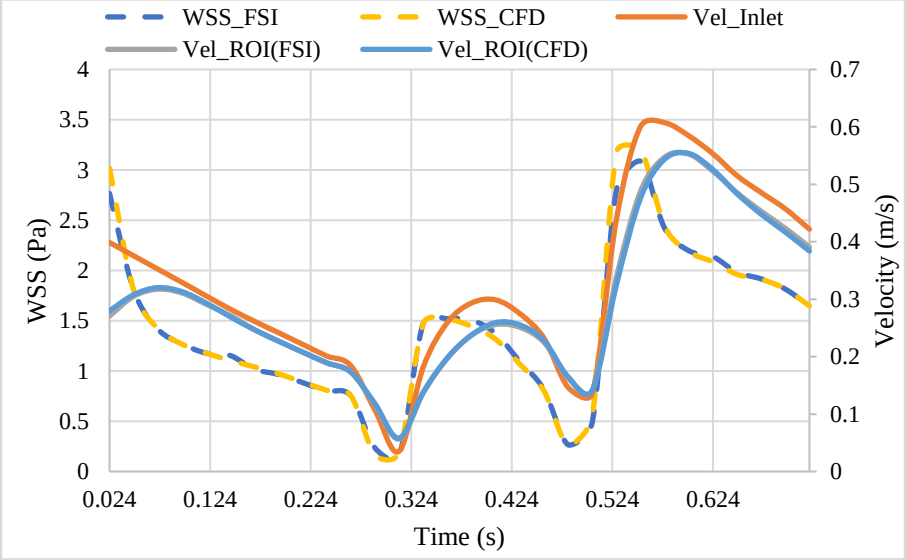

Figure 32. The Velocity and WSS Distribution of FSI and CFD under 13332 Pa Outlet Pressure

The contour plots of WSS distribution and TAWSS distribution computed by FSI and CFD using 0-gauge pressure outlet and constant 13332 (100 mmHg) Pa outlet are shown below. Only the contour plots of stented coronary artery are provided here. The maximum WSS is located at the surface of stent strut. Low WSS areas are spotted around the stent strut.

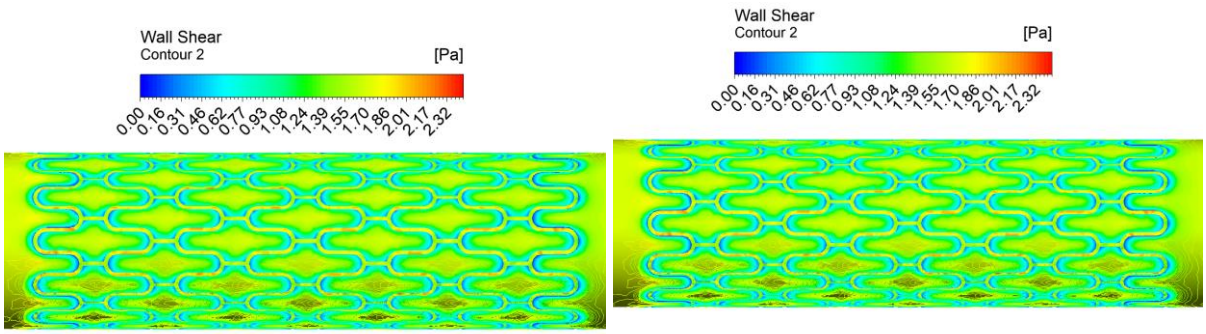

(a) **(b)**

Figure 33. The WSS Contour Plots of Stented Coronary Artery of CFD: (a) 0 Pa Outlet; (b) 13332Pa Outlet

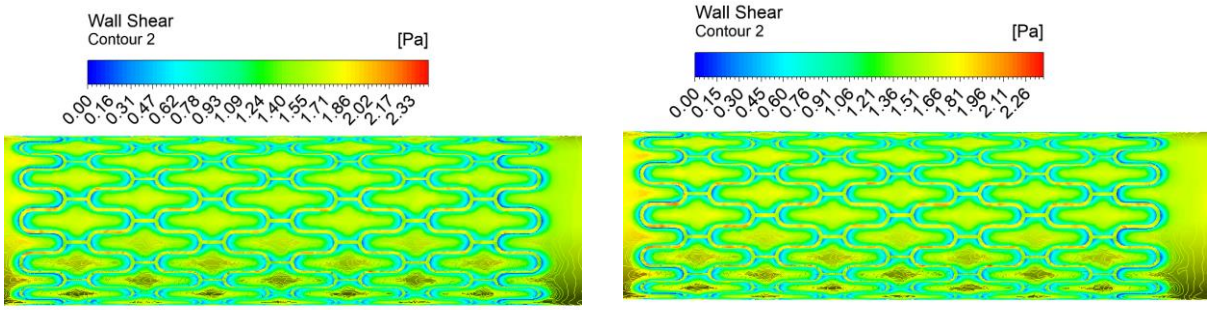

(a) **(b)**

Figure 34 . The WSS Contour Plots of Stented Coronary Artery of FSI: (a) 0 Pa Outlet; (b) 13332Pa Outlet

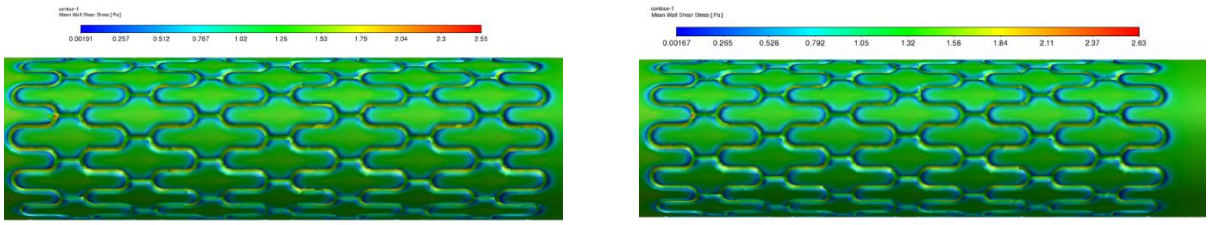

(a) **(b)**

Figure 35. The TAWSS Contour Plots of Stented Coronary Artery of CFD: (a) 0 Pa Outlet; (b) 13332Pa Outlet

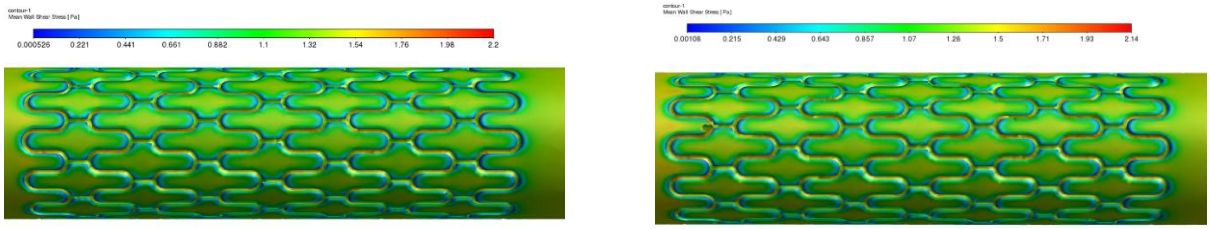

(a) **(b)**

Figure 36. The TAWSS Contour Plots of Stented Coronary Artery of FSI: (a) 0 Pa Outlet; (b) 13332Pa Outlet

According to the results in the table 6, it can be seen that when the outlet is set to 0-gauge pressure, there is no difference between using FSI and CFD to analyze the hemodynamics of idealized coronary artery. Based on table 6, the maximum WSS computed using outlet of 13332 Pa (100 mmHg) shows a minor variation which is approximately 2.6%. However, TAWSS shows a relatively high variation which is 18.1%. Hence, the results conclude that using CFD for investigating the WSS of idealized straight coronary artery is adequate.

Table 6. The Results and the General Description of 8 Numerical Models.

Number	Simulation Type	Geometry Description	Inlet Boundary Condition	Outlet Boundary Condition	Maximum WSS at 0.72s (Pa)	Maximum TAWSS at 0.72s (Pa)
1	CFD	Non-stented	Pulsatile parabolic blood profile	0-gauge	1.81	1.54
2	CFD	Non-stented	Pulsatile parabolic blood profile	Constant 13332 Pa	1.81	1.54
3	CFD	Stented	Pulsatile parabolic blood profile	0-gauge	2.32	2.63
4	CFD	Stented	Pulsatile parabolic blood profile	Constant 13332 Pa	2.32	2.55
5	FSI	Non-stented	Pulsatile parabolic blood profile	0-gauge	2.02	1.50
6	FSI	Non-stented	Pulsatile parabolic blood profile	Constant 13332 Pa	1.92	1.53
7	FSI	Stented	Pulsatile parabolic blood profile	0-gauge	2.32	2.20
8	FSI	Stented	Pulsatile parabolic blood profile	Constant 13332 Pa	2.26	2.14

4.2 The Results of Stented and Non-Stented Idealized Coronary Artery Bifurcation

The general description of different numerical model, maximum WSS and TAWSS at 0.72 s are summarized in table 7, and the contour plots of WSS and TAWSS at 0.72 s are shown in figure 39 and 40. The theoretical blood velocity streamline and computational blood velocity streamline are illustrated in figure 37 and 38. By comparing with the diagram which can theoretically define the region where the atherosclerosis is prone to form, the computational results can perfectly match with it. This means that the numerical model is defined correctly. Due to flow separation, when blood flows through the outer wall of the bifurcation, the transformation from laminar blood flow into turbulent blood flow occurs. This will result in

the recirculation zone which will finally lead to the low WSS area. In idealized coronary bifurcation, this phenomenon can be correctly captured using FSI simulation. Although FSI method can capture this phenomenon, the size of the oscillatory area is overestimated. In the (c) and (d) in figure 38 which are computed using CFD method, the turbulent blood flow is not captured.

By the results stated in figure 38, the velocity magnitude of CFD is higher than that of FSI. This is consisted to the findings in section 4.1.

Due to the different boundary condition and structure of arterial layer, the value of WSS and TAWSS could be different. By comparing the results between CFD and FSI, the WSS and TAWSS of CFD are significantly higher. The maximum WSS and TAWSS are spotted at the apex of bifurcation. This is because the impingement of blood flow can generate a higher velocity gradient there. The velocity at the outlet is overestimated by CFD. In (c) and (d) of figure 39, the WSS show abnormal high value around the outlet.

The WSS and TAWSS results of three-layered bifurcation and one-layered bifurcation show small deviation (1.3%). This indicates that one-layered arterial wall structure is sufficient for analyzing idealized coronary artery bifurcation.

The upstream flow velocity of the bifurcation is reduced due to the influence of stent. Therefore, the WSS and TAWSS near the downstream bifurcation are lower than those without stent.

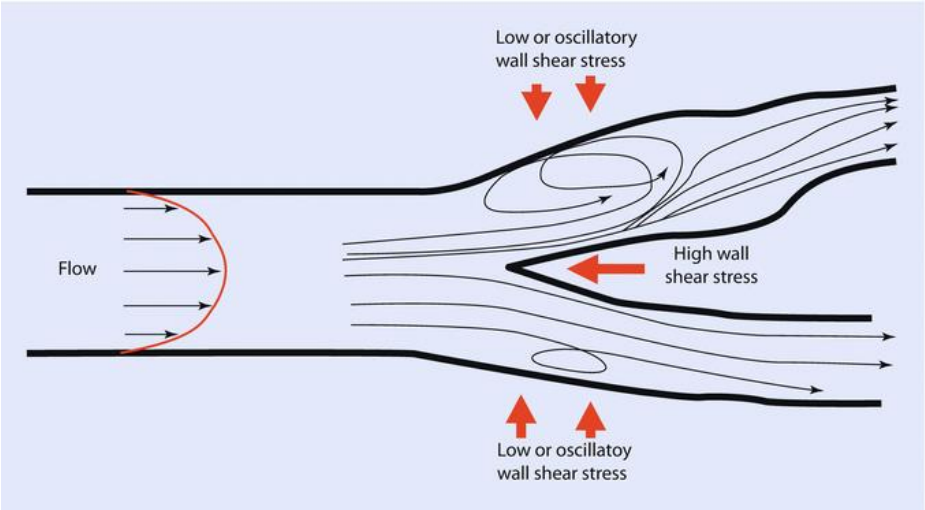

Figure 37. The Theoretical Hemodynamic Analysis of Coronary Artery Bifurcation. [44]

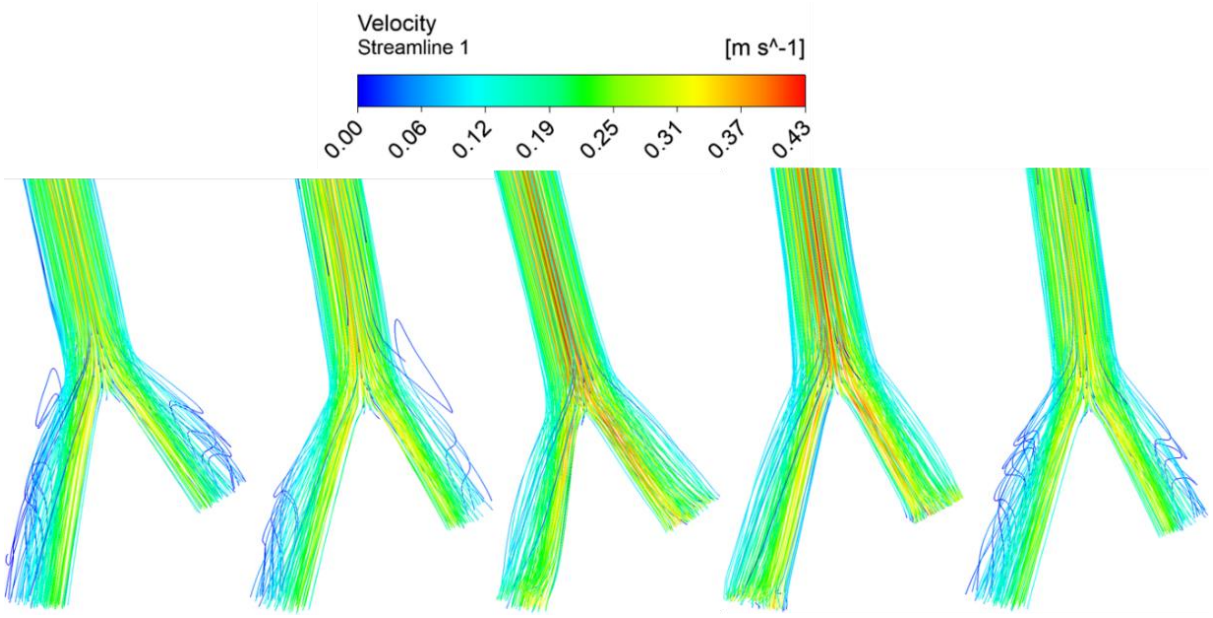

(a) (b) (c) (d) (e)

Figure 38. The Velocity Streamline of (a) FSI-One-Layered-Stented-Isotropic; (b) FSI-One-Layered-Non-Stented-Isotropic; (c) CFD-Stented; (d) CFD-Non-Stented; (e) FSI-Three-Layered-Isotropic

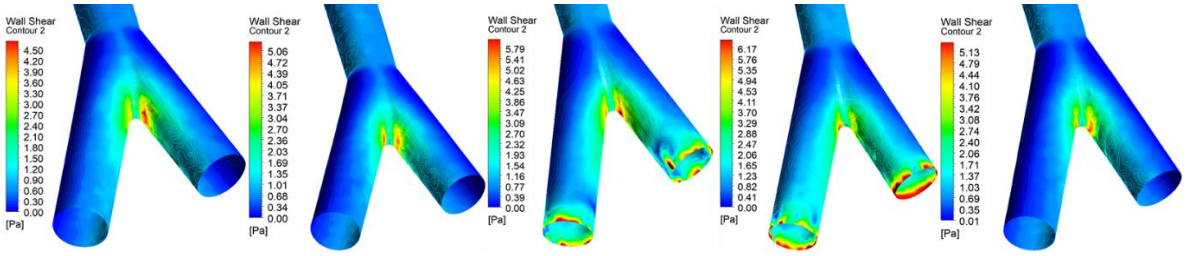

(a) (b) (c) (d) (e)

Figure 39. The WSS Contour Plots of (a) FSI-One-layered-Stented-Isotropic; (b) FSI-One-Layered-Non-Stented-Isotropic; (c) CFD-Stented; (d) CFD-Non-Stented; (e) FSI-Three-Layered-Isotropic

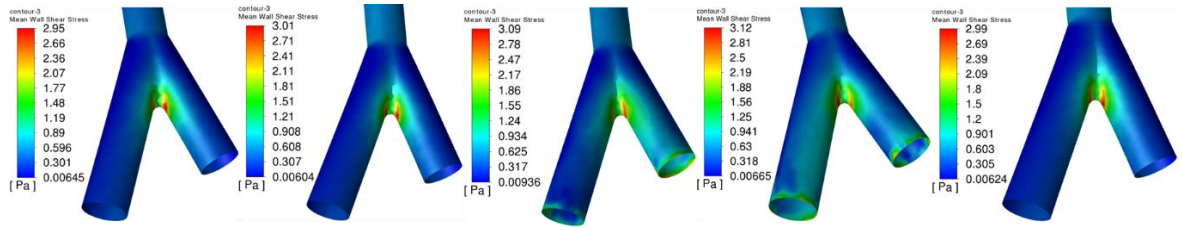

(a) (b) (c) (d) (e)

Figure 40. The TAWSS Contour Plots of (a) FSI-One-Layered-Stented-Isotropic; (b) FSI-One-layered-NonStented-Isotropic; (c) CFD-Stented; (d) CFD-Non-Stented; (e) FSI-Three-Layered- Non-Stented-Isotropic

Table 7. The Results and The General Description of 6 Numerical Models.

Number	Simulation Type	Geometry Description	Arterial Wall Structure	Material Model	Maximum WSS at 0.72s (Pa)	Maximum TAWSS at 0.72s (Pa)
1	FSI	Non-stented	One-layered	Isotropic Hyperelastic	5.06	2.95
2	FSI	Non-stented	Three-layered	Isotropic Hyperelastic	5.13	2.99
3	FSI	Stented	One-layered	Isotropic Hyperelastic	4.50	2.77
4	FSI	Stented	Three-layered	Isotropic Hyperelastic	Na	Na
5	CFD	Stented	Na	Na	5.79	3.09
6	CFD	Non-stented	Na	Na	6.17	3.12

4.3 The Results of Non-Stented Patient Specific Coronary Artery Bifurcation

Based on the foundation of first and second stage simulations, several simulations of patient specific bifurcation have been conducted. The general description of different numerical model, maximum WSS and TAWSS results are summarized in table 8.

Comparing results shown in figure 41, both FSI and CFD successfully capture the oscillatory and helical flow around the shoulder of bifurcation area where the atherosclerosis is prone to form. Similar to the results in 4.2, CFD method overestimates the blood velocity, WSS and TAWSS. According to the (e) in figure 41, the maximum WSS does not appear at the apex of the bifurcation. Additionally, the low WSS area on the left side branch is over-defined. These are different with the rest of results. In addition to this, the rest of contour plots of WSS and TAWSS distribution adequately match with the theoretical hemodynamic analysis.

The difference between the WSS computed using three-layered arterial wall structure and WSS computed using one-layered arterial wall structure is around 5%. This is slightly different from the previous results. The gap of TAWSS is around 2%.

Similarly, the deviation between the WSS of anisotropic material model and isotropic material model is approximately 5%. The difference of TAWSS is about 2%.

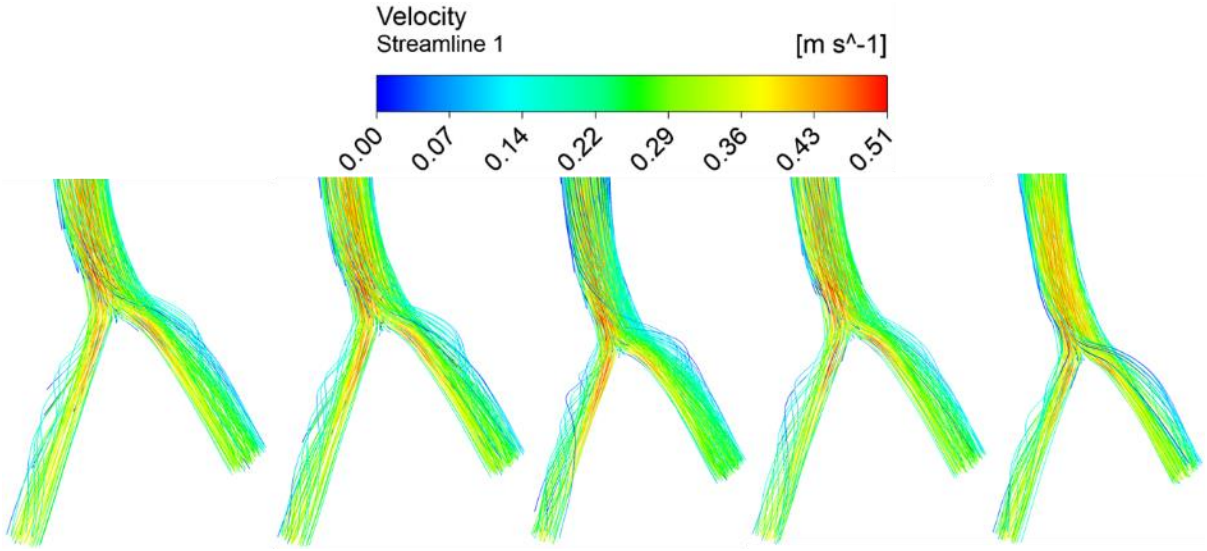

(a) (b) (c) (d) (e)

Figure 41. The Velocity Streamline Plots of (a) FSI-Three-Layered-Isotropic; (b) FSI-Three-Layered-Anisotropic; (c) CFD-Non-Stented; (d) FSI-One-Layered-Isotropic; (e) FSI-One-Layered-Anisotropic

The contour plots of WSS and TAWSS at 0.72 s and figure 42 and 43 below.

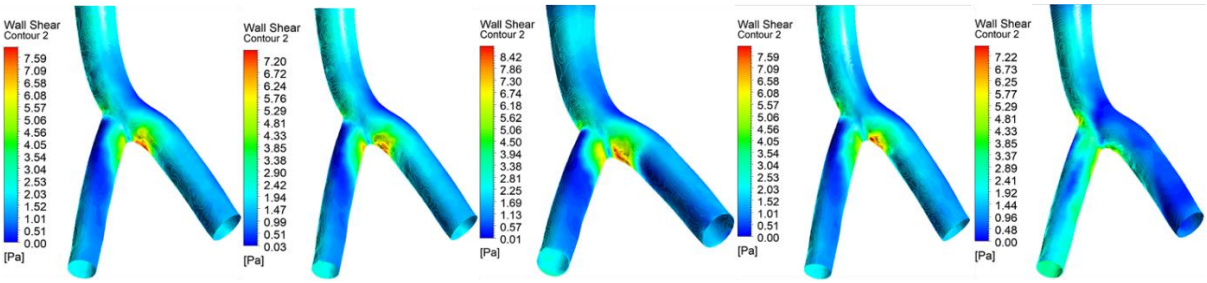

(a) (b) (c) (d) (e)

Figure 42. The WSS Contour Plots of (a) FSI-Three-layered-Isotropic; (b) FSI-Three-Layered-Anisotropic; (c) CFD-Non-Stented; (d) FSI-One-Layered-Isotropic; (e) FSI-One-Layered-Anisotropic

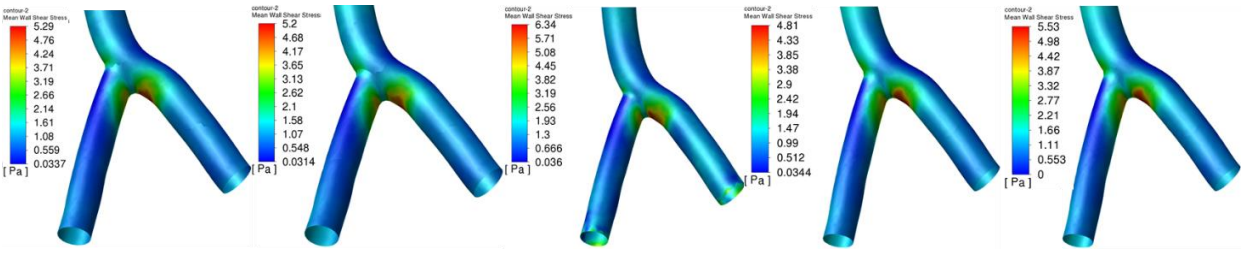

(a) (b) (c) (d) (e)

Figure 43. The TAWSS Contour Plots of (a) FSI-Three-Layered-Isotropic; (b) FSI-Three-Layered-Anisotropic; (c) CFD- Non-Stented; (d) FSI-One-layered-Isotropic; (e) FSI-One-Layered-Anisotropic

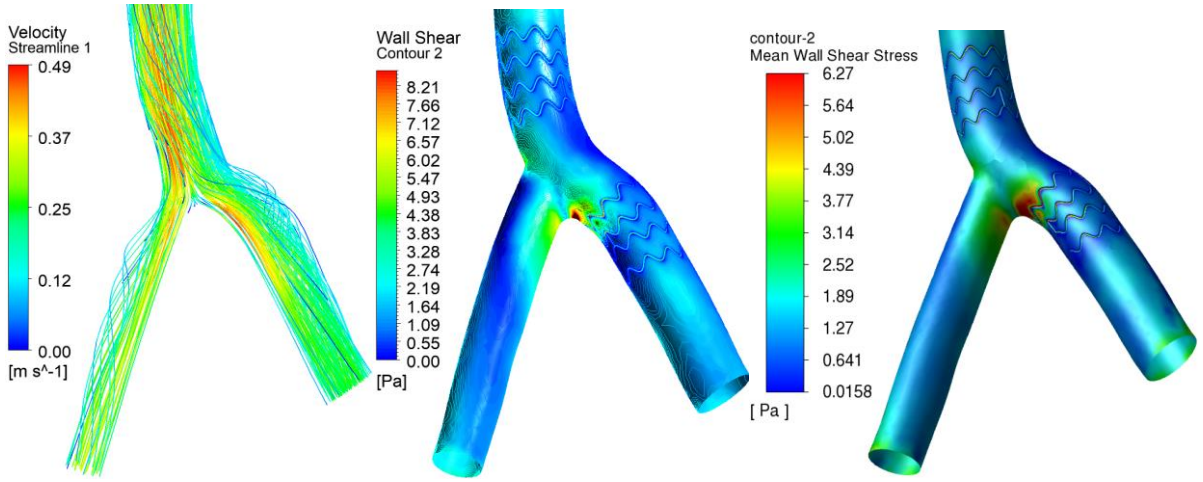

(a) **(b)** **(c)**

Figure 44. (a) The Velocity Streamline Plots of CFD-Stented; (b) The WSS Contour Plots of CFD-Stented; (c) The TAWSS Contour Plots of CFD-Stented

Table 8. The Results and The General Description of 8 Numerical Models.

Number	Simulation Type	Geometry Description	Arterial Wall Structure	Material Model	Maximum WSS at 0.72s (Pa)	Maximum TAWSS at 0.72s (Pa)
1	FSI	Non-stented	One-layered	Isotropic Hyperelastic	7.59	5.3
2	FSI	Non-stented	Three-layered	Anisotropic Hyperelastic	7.59	5.29
3	FSI	Non-stented	One-layered	Anisotropic Hyperelastic	7.22	5.53
4	FSI	Non-stented	Three-layered	Isotropic Hyperelastic	7.20	5.20
5	FSI	Stented	One-layered	Anisotropic Hyperelastic	Na	Na
6	FSI	Stented	Three-layered	Isotropic Hyperelastic	Na	Na
7	CFD	Non-stented	Na	Na	8.42	6.34
8	CFD	Stented	Na	Na	8.21	6.27

Chapter 5 – Discussion

The purpose of this project is to construct a more realistic and accurate numerical model for evaluating hemodynamics of coronary artery. Therefore, it is necessary to understand the factors that affect the hemodynamic results.

5.1 The Influence of Outlet Boundary Condition on Arterial Hemodynamics

Most of the current study are using the velocity-pressure coupling method to conduct the CFD or FSI simulation for evaluating the hemodynamics of coronary artery [21, 45, 46]. This is because the inlet blood velocity magnitude and inlet blood prefile can be measured using pulsatile flow tracing device. The velocity-pressure coupling is a robust method which is widely used in FLUENT. Blood pressure is the main factor leading to the deformation of arterial wall. It is produced when blood is pumped by the heart into the arteries. In the first stage of this study, the results exhibit that when the outlet is set to 0-gauge pressure, there is no difference between FSI and CFD to analyze the hemodynamics of idealized straight coronary artery. When the outlet is set to 0 pressure, the blood pressure in the whole vascular cavity will be caused only by blood flow. At this time, the value of blood pressure on the arterial wall can only reach hundreds of Pa. This is different from the real blood pressure in the human body. In this case, the arterial wall will hardly deform. Therefore, 0-gauge pressure outlet is an unreasonable boundary conditions when conducting FSI simulation. Although the constant average blood pressure outlet can provide more reasonable hemodynamic results, it cannot describe the hemodynamic phenomenon during the systole and diastole. Hence, pulsatile pressure profile outlet is necessary to capture the dynamic hemodynamic behavior during the cardiac cycle. This has been validated as the correct approach in Chiastra et al.'s publication [18].

5.2 The Influence of FSI on Arterial Hemodynamics

In the computational hemodynamic analysis, FSI is a method which can take the compliance of arterial wall into account. This means that the blood flow and arterial wall will form a dynamic system and they will interact with each other. In this study, the main difference between CFD and FSI is that FSI includes the variation of fluid domain caused by the deformation and compliance of arterial wall. The most crucial hemodynamic parameter is WSS. All the rest of parameters can be calculated based on it. By comparing the maximum WSS in chapter 4, the difference of idealized straight coronary artery is 2.6% which can match with the

results (1.5%) in Chiastra et al.'s publication [18]. For patient specific bifurcation, the error of WSS between CFD and FSI is 13.7%. This is consisted with the difference (11%) in Malvè et al.'s study [14]. However, for idealized coronary artery bifurcation, the difference of WSS between CFD and FSI is 20.1% which is a relatively large. This is because the over-predicted oscillatory blood flow around the apex of bifurcation negatively impacts the normal blood flow near the maximum WSS area. This can be spotted in figure 39, 40, 42 and 43. According to the figure 45, the influence of radius, velocity and viscosity on WSS can be illustrated. Under the condition of same speed and viscosity, the WSS will only be affected by the inner diameter of the coronary artery. The inner diameter of the coronary artery in FSI is larger than that in CFD, due to the consideration of the compliance and deformation of arterial wall caused by blood pressure. Hence, the velocity and WSS computed using FSI are smaller than those computed by CFD. This finding can match with the conclusion in M. Malvè et al. and Lopes et al.'s study [14,39].

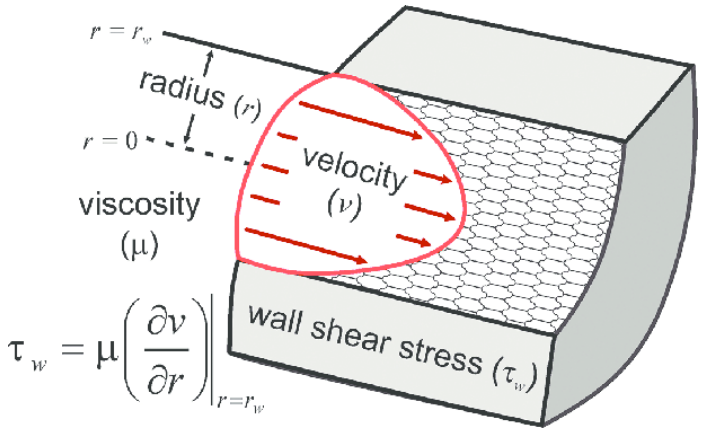

Figure 45. The Definition of WSS [47]

5.3 The influence of Three-Layered arterial wall structure on arterial hemodynamics

Arterial wall is formed by three layers which have different mechanical properties [23]. In this study, the FSI and CFD simulation with both three-layered and one-layered coronary artery bifurcation are conducted. The results show that the consideration of three-layered arterial wall structure slightly affect WSS and TAWSS. However, under the same mesh settings, the computational time of three-layered numerical model is significantly increased. This is due to the introduction of contact between the intima, media and adventitia in solid domain. When the intima is deformed by blood pressure, the force will be transmitted from the intima to the media

through the defined contact surface, and finally from the media to the adventitia.

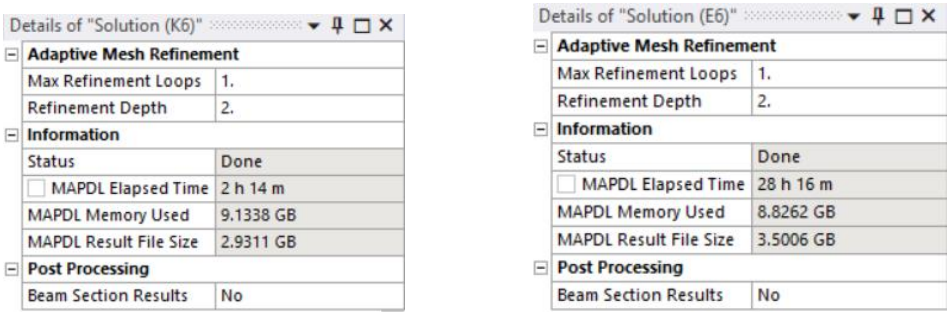

Details of "Solution (K6)"

Adaptive Mesh Refinement	
Max Refinement Loops	1.
Refinement Depth	2.
Information	
Status	Done
MAPDL Elapsed Time	2 h 14 m
MAPDL Memory Used	9.1338 GB
MAPDL Result File Size	2.9311 GB
Post Processing	
Beam Section Results	No

Details of "Solution (E6)"

Adaptive Mesh Refinement	
Max Refinement Loops	1.
Refinement Depth	2.
Information	
Status	Done
MAPDL Elapsed Time	28 h 16 m
MAPDL Memory Used	8.8262 GB
MAPDL Result File Size	3.5006 GB
Post Processing	
Beam Section Results	No

(a) **(b)**

Figure 46. The Computational Time of (a) One-Layered Arterial Wall Structure; (b) Three-Layered Arterial Wall Structure.

5.4 The Influence of Anisotropic Hyperelastic Material on Arterial Hemodynamics

The anisotropy is a crucial characteristic of arterial wall. This anisotropy is mainly reflected in the longitudinal and circumferential stiffness of each arterial layer. The reason for this anisotropy is that there are collagen fibers distributed in different directions in the media and adventitia. By comparing the WSS and TAWSS results obtained using anisotropic and isotropic material models, there is almost no difference between these two hemodynamic parameters. As can be seen from figure 26 (a), when the strain of the blood vessel is in a relatively small stage, such as diastole, the stiffness of each arterial layer is very small. At this time, the mechanical properties of each arterial layer are dominated only by the elastic arterial wall matrix (endothelial cells and elastin) [48]. In systole, the maximum blood pressure on the arterial wall is 16000 Pa (120 mmHg). Under this condition, due to the increase of the circumferential stress of the arterial wall, the collagen fibers in the arterial wall will be fully stretched and then dominate the mechanical behavior of the arterial wall. Therefore, the stiffness of arterial wall will significantly increase to ensure that the coronary artery will not be torn. In this project, the maximum blood pressure of 16000 Pa (120 mmHg) was reached only when the time step was 0.408 seconds during one cardiac cycle. These phenomena can be described in figure 47. Therefore, most of the time, the mechanical behavior of the arterial wall can be considered as isotropic hyperelasticity. Therefore, there is no significant gap in the hemodynamic results obtained by simulations using isotropic and anisotropic hyperelastic material model.

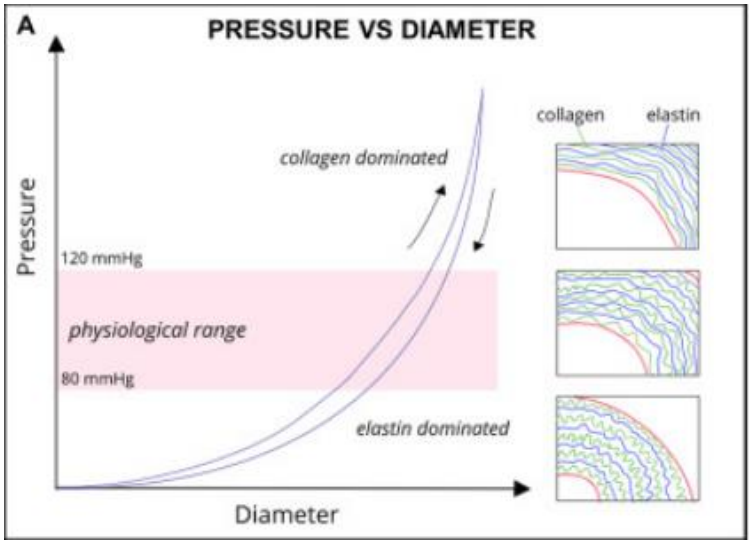

Figure 47. The Physiological Mechanical Behavior of Arterial Wall [48]

5.5 The influence of Geometry on Arterial Hemodynamics

FSI and CFD simulations are carried out for the three geometries. By comparing parent specific and idealized bifurcation, it can be found that the blood velocity, WSS and TAWSS of patient specific geometry are higher than those of idealized geometry. This is because in real life, the diameter of coronary artery cannot remain constant, and the diameter of bifurcation in patient specific model has changed. Moreover, the diameter of two branches is also smaller than that of the main branch, resulting in higher blood velocity, WSS and TAWSS. In the R&D of cardiovascular devices, the use of idealized coronary artery to analyze hemodynamics in the early stage can provide engineers with a general guidance. This can greatly shorten the product development cycle. However, in later clinical trials, it is necessary to use patient specific coronary artery to assist the optimization of cardiovascular devices. Because the complex curved surface in the patient specific model is usually the high incidence region of atherosclerosis, and this region may be oversimplified and ignored in the idealized model. Therefore, in order to obtain realistic and accurate hemodynamic analysis results, it is very important to correctly define the geometric model of coronary artery.

5.6 The Influence of Stent on Arterial Hemodynamics

According to figure 48, when the stent is present in the coronary artery, the hemodynamics at the stent is affected. This is reflected in the low WSS area near the support strut. There is also a high WSS area on the surface of stent strut. This can be confirmed by these articles [10, 18].

High WSS areas can lead to the rupture of unstable plaques, causing acute thrombosis. Low WSS area will accelerate plaque growth and intimal hyperplasia. With the use of cylindrical section stent, the low WSS area near the stent strut is improved. This is because when the blood flows through the stent strut, the streamlined design can mitigate the flow separation which will lead to the recirculation zone. This can be confirmed in the study of koskinas et al. [6].

(a) **(b)**

Figure 48. The Stented Region: (a) Idealized Straight Coronary Artery; (b) Idealized Coronary Artery Bifurcation

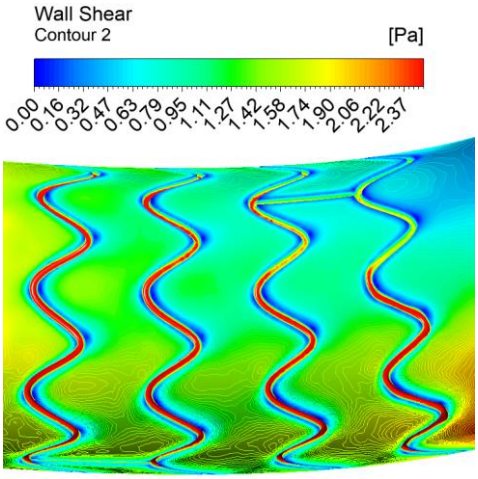

Figure 49. The Stented Region of Patient Specific Coronary Artery Bifurcation

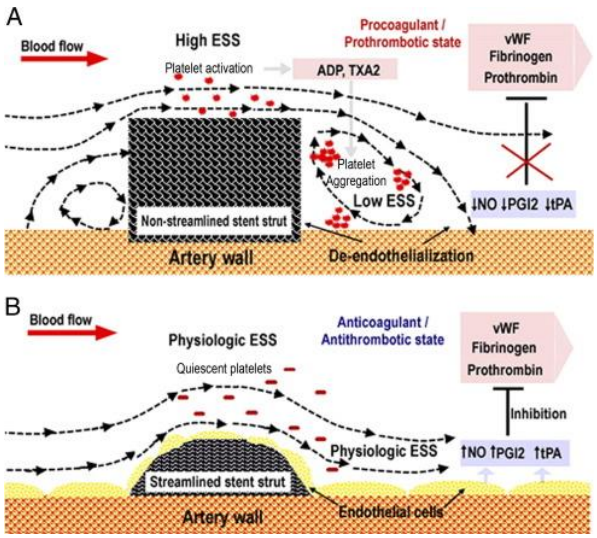

Figure 50. The Comparison Between Rectangular and Circular Stent Strut on Local Hemodynamics [6]

Chapter 6 - Conclusion

The aim of this project is to construct a more realistic and accuracy numerical model by analyzing different factors which can influence the computational results. The effect of outlet boundary condition, arterial wall deformation, material model of arterial wall and arterial wall structure on the hemodynamic parameters are evaluated. Idealized straight coronary, idealized coronary artery bifurcation and patient specific coronary bifurcation are simulated using CFD and FSI method. By constructing stent into these geometries, the effect of stent on hemodynamic parameters is also investigated. The results conclude that inlet pulsatile parabolic blood velocity profile and outlet pulsatile blood pressure profile are the most appropriate boundary conditions for conducting FSI simulation on analyzing arterial hemodynamics. FSI method can provide more realistic hemodynamic results, while these are overestimated by CFD method. The consideration of three-layered arterial wall does not affect the hemodynamic parameters. However, it will significantly increase the computational time. For analyzing the hemodynamics of coronary artery under the normal physiological conditions, isotropic hyperelastic material model is adequate. Anisotropic hyperelastic material model is more suitable to analyze the tissue with large deformation such as aortic valve and heart muscle. Geometry can significantly impact the hemodynamic results. In this study, the difference of WSS between idealized and patient specific bifurcation is approximately 31.1%. The most efficient method is to use idealized geometry as the general guidance and use patient specific geometry to obtain the results. Lastly, the present of stent has an impact on both local and global hemodynamics. In conclusion, this study provides a FSI framework of realistic numerical modelling for the R&D engineers of cardiovascular devices to evaluate and optimize their products. It can also assist doctor to quantify the development and condition of atherosclerosis in patients.

Chapter 7 – Limitation and Future Works

Although this project has created relatively realistic and accurate numerical models and analyzed the hemodynamic results obtained through these models, there are still some factors which are neglected. The first one is the arterial wall motion induced by heart beating. Another one is the consideration of plaque.

7.1 Future Work of The Consideration of Heart Motion

The coronary arteries are usually fitted or embedded on the surface of the heart. The Myocardial relaxation and contraction will greatly affect its hemodynamics and wall deformation. The heart motion can be modeled in solid domain by applying a transient force varying with the cardiac cycle.

7.2 Future Work of The Anisotropic Material Model

The current anisotropic hyperelastic material model defined by ANSYS APDL created by the author can be used to conduct FSI simulations by using. However, unlike those two geometries, the patient specific coronary artery bifurcation is highly irregular with a changing centerline and diameter of arterial wall. Hence, every element created by the meshing operation will have its unique local cylindrical coordinate system. This should be included in the ANSYS APDL code in the future.

7.3 Future Work of The Consideration of Arterial Plaque

The current numerical model can accurately analyze the hemodynamics of healthy coronary artery. However, the hemodynamics around atherosclerotic lesions is more complex. Therefore, it is meaningful to analyze the coronary artery with plaque or even coronary bifurcation with plaque. In order to achieve this, the consideration of the material of plaque and the construction of geometry is significant. Constructing stent at plaque for FSI simulation may provide more realistic hemodynamic results. The current numerical model can be the foundation to guide this work.

7.4 Future Work of The Unfinished Simulation

Due to the limitation of RAMs of the workstation, there are total three numerical models in this project which are not completed using FSI. They are idealized three-layered coronary artery bifurcation with stent, patient specific one-layered coronary artery bifurcation with stent and patient specific three-layered coronary artery bifurcation with stent. All these numerical models

have been correctly built. The student who will undertake this project can continue to finish these models using the HPC of UNSW with the requirement of more cores and RAMs.

References

[1] World Health Organisation, “WHO | About cardiovascular diseases,” *Who.int*, Sep. 2011, doi: /entity/cardiovascular_diseases/about_cvd/en/index.html.

[2] A. J. Lusis, “Atherosclerosis,” *Nature*, vol. 407, no. 6801, pp. 233–241, Sep. 2000, doi: 10.1038/35025203.

[3] B. R. Kwak *et al.*, “Biomechanical factors in atherosclerosis: mechanisms and clinical implications,” *European Heart Journal*, vol. 35, no. 43, pp. 3013–3020, Sep. 2014, doi: 10.1093/eurheartj/ehu353.

[4] K. Marker, “Building New Routes for Surgical Stents and Artery Repair | Cardiology,” *Labroots*, Jan. 05, 2017. https://www.labroots.com/trending/cardiology/4977/building-routes-surgical-stents-artery-repair (accessed Apr. 21, 2021).

[5] L Pleva, P Kukla, and O Hlinomaz. “Treatment of coronary in-stent restenosis: a systematic review,” *J Geriatr Cardiol*, vol. 15, no. 2, pp. 173-184, Feb 2018, doi: 10.11909/j.issn.1671-5411.2018.02.007.

[6] K. C. Koskinas, Y. S. Chatzizisis, A. P. Antoniadis, and G. D. Giannoglou, “Role of Endothelial Shear Stress in Stent Restenosis and Thrombosis,” *Journal of the American College of Cardiology*, vol. 59, no. 15, pp. 1337–1349, Apr. 2012, doi: 10.1016/j.jacc.2011.10.903.

[7] T. Inoue, K. Croce, T. Morooka, M. Sakuma, K. Node, and D. I. Simon, “Vascular Inflammation and Repair,” *JACC: Cardiovascular Interventions*, vol. 4, no. 10, pp. 1057–1066, Oct. 2011, doi: 10.1016/j.jcin.2011.05.025.

[8] T. Gori, A. Polimeni, C. Indolfi, L. Räber, T. Adriaenssens, and T. Münzel, “Predictors of stent thrombosis and their implications for clinical practice,” *Nature Reviews. Cardiology*, vol. 16, no. 4, pp. 243–256, Apr. 2019, doi: 10.1038/s41569-018-0118-5.

[9] L. Wei, H. L. Leo, Q. Chen, and Z. Li, “Structural and Hemodynamic Analyses of Different Stent Structures in Curved and Stenotic Coronary Artery,” *Frontiers in Bioengineering and Biotechnology*, vol. 7, Dec. 2019, doi: 10.3389/fbioe.2019.00366.

[10] S. Beier *et al.*, “Hemodynamics in Idealized Stented Coronary Arteries: Important Stent Design Considerations,” *Annals of Biomedical Engineering*, vol. 44, no. 2, pp. 315–329, Jul. 2015, doi: 10.1007/s10439-015-1387-3.

[11] H. Samady *et al.*, “Coronary Artery Wall Shear Stress Is Associated With Progression and Transformation of Atherosclerotic Plaque and Arterial Remodeling in Patients With Coronary Artery Disease,” *Circulation*, vol. 124, no. 7, pp. 779–788, Aug. 2011, doi: 10.1161/circulationaha.111.021824.

[12] M. Ahamed, S. Atique, M. Munshi, and T. Koiranen, “A Concise Description of One Way and Two Way Coupling Methods for Fluid-Structure Interaction Problems,” *American Journal of Engineering Research (AJER)*, vol. 6, no. 3, pp. 86–89, 2017.

[13] D. Lopes, H. Puga, J. Teixeira, and R. Lima, “Blood flow simulations in patient-specific geometries of the carotid artery: A systematic review,” *Journal of Biomechanics*, vol. 111, p. 110019, Oct. 2020, doi: 10.1016/j.jbiomech.2020.110019.

[14] M. Malvè, A. García, J. Ohayon, and M. A. Martínez, “Unsteady blood flow and mass transfer of a human left coronary artery bifurcation: FSI vs. CFD,” *International Communications in Heat and Mass Transfer*, vol. 39, no. 6, pp. 745–751, Jul. 2012, doi: 10.1016/j.icheatmasstransfer.2012.04.009.

[15] P. K. Siogkas *et al.*, “Patient-Specific Simulation of Coronary Artery Pressure Measurements: AnIn VivoThree-Dimensional Validation Study in Humans,” *BioMed Research International*, vol. 2015, pp. 1–11, 2015, doi: 10.1155/2015/628416.

[16] M. Cilla, I. Borrás, E. Peña, M. A. Martínez, and M. Malvè, “A parametric model for analysing atherosclerotic arteries: On the FSI coupling,” *International Communications in Heat and Mass Transfer*, vol. 67, pp. 29–38, Oct. 2015, doi: 10.1016/j.icheatmasstransfer.2015.06.017.

[17] W. Lee, S. W. Cho, U. K. Allahwala, and R. Bhindi, “Numerical study to identify the effect of fluid presence on the mechanical behavior of the stents during coronary stent expansion,” *Computer Methods in Biomechanics and Biomedical Engineering*, vol. 23, no. 11, pp. 744–754, May 2020, doi: 10.1080/10255842.2020.1763967.

[18] C. Chiastra, F. Migliavacca, M. Á. Martínez, and M. Malvè, “On the necessity of modelling fluid–structure interaction for stented coronary arteries,” *Journal of the Mechanical Behavior of Biomedical Materials*, vol. 34, pp. 217–230, Jun. 2014, doi: 10.1016/j.jmbbm.2014.02.009.

[19] T. Chaichana, Z. Sun, and J. Jewkes, “Computation of hemodynamics in the left coronary artery with variable angulations,” *Journal of Biomechanics*, vol. 44, no. 10, pp. 1869–1878, Jul. 2011, doi: 10.1016/j.jbiomech.2011.04.033.

[20] V. Carvalho, D. Pinho, R. A. Lima, J. C. Teixeira, and S. Teixeira, “Blood Flow Modeling in Coronary Arteries: A Review,” *Fluids*, vol. 6, no. 2, p. 53, Jan. 2021, doi: 10.3390/fluids6020053.

[21] V. Kashyap, B. B. Arora, and S. Bhattacharjee, “A computational study of branch-wise curvature in idealized coronary artery bifurcations,” *Applications in Engineering Science*, vol. 4, p. 100027, Dec. 2020, doi: 10.1016/j.apples.2020.100027.

[22] A. Gholipour, M. H. Ghayesh, A. Zander, and R. Mahajan, “Three-dimensional biomechanics of coronary arteries,” *International Journal of Engineering Science*, vol. 130, pp. 93–114, Sep. 2018, doi: 10.1016/j.ijengsci.2018.03.002.

[23] G. A. Holzapfel, T. C. Gasser, and R. W. Ogden, “A New Constitutive Framework for Arterial Wall Mechanics and a Comparative Study of Material Models,” *Journal of Elasticity*, vol. 61, no. 1/3, pp. 1–48, 2000, doi: 10.1023/a:1010835316564.

[24] D. Meza, D. A. Rubenstein, and W. Yin, "A Fluid–Structure Interaction Model of the Left Coronary Artery," *Journal of Biomechanical Engineering*, vol. 140, no. 12, Sep. 2018, doi: 10.1115/1.4040776.

[25] L. Kallekar, C. Viswanath, and M. Anand, "Effect of Wall Flexibility on the Deformation during Flow in a Stenosed Coronary Artery," *Fluids*, vol. 2, no. 2, p. 16, Apr. 2017, doi: 10.3390/fluids2020016.

[26] P. Tricerri, L. Dedè, S. Deparis, A. Quarteroni, A. M. Robertson, and A. Sequeira, "Fluid-structure interaction simulations of cerebral arteries modeled by isotropic and anisotropic constitutive laws," *Computational Mechanics*, vol. 55, no. 3, pp. 479–498, Jan. 2015, doi: 10.1007/s00466-014-1117-y.

[27] D. Zeng, E. Boutsianis, M. Ammann, K. Boomsma, S. Wildermuth, and D. Poulikakos, "A Study on the Compliance of a Right Coronary Artery and Its Impact on Wall Shear Stress," *Journal of Biomechanical Engineering*, vol. 130, no. 4, Jun. 2008, doi: 10.1115/1.2937744.

[28] A. Theodorakakos *et al.*, "Simulation of cardiac motion on non-Newtonian, pulsating flow development in the human left anterior descending coronary artery," *Physics in Medicine and Biology*, vol. 53, no. 18, pp. 4875–4892, Aug. 2008, doi: 10.1088/0031-9155/53/18/002.

[29] A. Razavi, E. Shirani, and M. R. Sadeghi, "Numerical simulation of blood pulsatile flow in a stenosed carotid artery using different rheological models," *Journal of Biomechanics*, vol. 44, no. 11, pp. 2021–2030, Jul. 2011, doi: 10.1016/j.jbiomech.2011.04.023.

[30] B. M. Johnston, P. R. Johnston, S. Corney, and D. Kilpatrick, "Non-Newtonian blood flow in human right coronary arteries: steady state simulations," *Journal of Biomechanics*, vol. 37, no. 5, pp. 709–720, May 2004, doi: 10.1016/j.jbiomech.2003.09.016.

[31] M. H. Amiri, A. Keshavarzi, A. Karimipour, M. Bahiraei, M. Goodarzi, and J. A. Esfahani, "A 3-D numerical simulation of non-Newtonian blood flow through femoral artery bifurcation with a moderate arteriosclerosis: investigating Newtonian/non-Newtonian flow and its effects on elastic vessel walls," *Heat and Mass Transfer*, vol. 55, no. 7, pp. 2037–2047, Feb. 2019, doi: 10.1007/s00231-019-02583-4.

[32] N. Kumar, A. Khader, R. Pai, P. Kyriacou, S. Khan, and P. Koteshwara, "Computational fluid dynamic study on effect of Carreau-Yasuda and Newtonian blood viscosity models on hemodynamic parameters," *Journal of Computational Methods in Sciences and Engineering*, vol. 19, no. 2, pp. 465–477, May 2019, doi: 10.3233/jcm-181004.

[33] A. Mahalingam *et al.*, "Numerical analysis of the effect of turbulence transition on the hemodynamic parameters in human coronary arteries," *Cardiovascular Diagnosis and Therapy*, vol. 6, no. 3, pp. 208–220, Jun. 2016, doi: 10.21037/cdt.2016.03.08.

[34] M. Biglarian *et al.*, "Computational investigation of stenosis in curvature of coronary artery within both dynamic and static models," *Computer Methods and Programs in Biomedicine*, vol. 185, p. 105170, Mar. 2020, doi: 10.1016/j.cmpb.2019.105170.

[35] J. Ryval, A. G. Straatman, and D. A. Steinman, “Two-equation Turbulence Modeling of Pulsatile Flow in a Stenosed Tube,” *Journal of Biomechanical Engineering*, vol. 126, no. 5, pp. 625–635, Oct. 2004, doi: 10.1115/1.1798055.

[36] “CV Physiology | Turbulent Flow,” *www.cvphysiology.com*, Jan. 03, 2018. https://www.cvphysiology.com/Hemodynamics/H007.

[37] I. ANSYS, *ANSYS Fluent User’s Guide*, R1 ed. Canonsburg, PA: ANSYS, Inc. and ANSYS Europe, Ltd, 2021, pp. 1576–1620.

[38] L. Zouggari, B. Bou-said, F. Massi, A. Culla, and A. Millon, “The Role of Biomechanics in the Assessment of Carotid Atherosclerosis Severity: A Numerical Approach,” *World Journal of Vascular Surgery*, vol. 1, no. 1, Mar. 2018

[39] D. Lopes, H. Puga, J. C. Teixeira, and S. F. Teixeira, “Influence of arterial mechanical properties on carotid blood flow: Comparison of CFD and FSI studies,” *International Journal of Mechanical Sciences*, vol. 160, pp. 209–218, Sep. 2019, doi: 10.1016/j.ijmecsci.2019.06.029.

[40] “Nitinol technical properties | Johnson Matthey,” *matthey.com*. https://matthey.com/en/products-and-services/medical-components/resource-library/nitinol-technical-properties.

[41] W. W. Nichols and D. A. Mcdonald, *McDonald’s blood flow in arteries : theoretic, experimental, and clinical principles*. London: Hodder Arnold, 2011.

[42] “CV Physiology | Laminar Flow,” *www.cvphysiology.com*, Jan. 03, 2018. https://www.cvphysiology.com/Hemodynamics/H006.

[43] M. Abbasian, M. Shams, Z. Valizadeh, A. Moshfegh, A. Javadzadegan, and S. Cheng, “Effects of different non-Newtonian models on unsteady blood flow hemodynamics in patient-specific arterial models with in-vivo validation,” *Computer Methods and Programs in Biomedicine*, vol. 186, p. 105185, Apr. 2020, doi: 10.1016/j.cmpb.2019.105185.

[44] M. Spaziano, Y. Louvard, and T. Lefèvre, “Treatment of Coronary Bifurcation Lesions,” in *Textbook of Catheter-Based Cardiovascular Interventions*, 225 b/w illustrations, 615 illustrations in colour: Springer, Cham, 2018, pp. 747–748.

[45] M. F. Rabbi, F. S. Laboni, and M. T. Arafat, “Computational analysis of the coronary artery hemodynamics with different anatomical variations,” *Informatics in Medicine Unlocked*, vol. 19, p. 100314, 2020, doi: 10.1016/j.imu.2020.100314.

[46] R. Jahromi, H. A. Pakravan, M. S. Saidi, and B. Firoozabadi, “Primary stenosis progression versus secondary stenosis formation in the left coronary bifurcation: A mechanical point of view,” *Biocybernetics and Biomedical Engineering*, vol. 39, no. 1, pp. 188–198, Jan. 2019, doi: 10.1016/j.bbe.2018.11.006.

[47] M. M. Samyn and J. F. LaDisa, “Novel Applications of Cardiovascular Magnetic Resonance Imaging-Based Computational Fluid Dynamics Modeling in Pediatric Cardiovascular and Congenital Heart Disease,” *Assessment of Cellular and Organ Function and Dysfunction using Direct and Derived MRI Methodologies*, Oct. 2016, doi: 10.5772/64814.

[48] D. B. Camasão and D. Mantovani, “The mechanical characterization of blood vessels and their substitutes in the continuous quest for physiological-relevant performances. A critical review,” *Materials Today Bio*, vol. 10, p. 100106, Mar. 2021, doi: 10.1016/j.mtbio.2021.100106.

Appendix

In order to understand the structure of the stent, the author designed and processed the prototype of the stent during his internship. The stent is manufactured by laser cutting a nickel-titanium tube. In order to understand the release process of the stent, the author watched the operation of a complete stent release system. The release process and manufactured Nitinol stent are show in figure 51 and 52.

Figure 51. The Release Process of Stent

Figure 52. The Stent Manufactured by Author